RNAi Screening of the Kinome Identifies PACT as a Novel Genetic Modifier of Foci Integrity in Myotonic Dystrophy type 1

Sean O'Reilly

Thesis submitted on Monday, September 30, 2013, to the Faculty of Medicine in partial fulfillment of the requirements for the M.Sc. in Cellular and Molecular Medicine

Cellular and Molecular Medicine

Faculty of Medicine

University of Ottawa

Abstract

Myotonic Dystrophy type 1 (DM1), the most common form of adult muscular dystrophy (~1:8000) currently has no effective treatment. In DM1, expansion of a tri-nucleotide repeat in the 3' UTR of the DMPK gene results in DMPK mRNA hairpin structures, aggregating as insoluble ribonuclear foci. The resulting mis-regulation of important splicing factors, causes the inclusion of fetal exons in dozens of transcripts that contribute to the disease phenotype (ClC-1: myotonia, IR: insulin resistance, and muscle wasting). In order to identify novel gene targets and kinase signalling pathways for potential therapeutics we have performed a high-throughput RNAi screen using an siRNA library targeting 518 protein kinases. RNA foci were visualized by in-situ hybridization of a fluorescently tagged probe to the expanded DMPK mRNA and the surface area and number of foci per nuclei were recorded. From our screen, we have identified a novel gene, PACT, as a modulator of foci integrity and that PACT knockdown can induce MBNL1 protein levels. The identified signalling complex represents a valid target for DM1 therapeutics considering its role in the modulation of the disease phenotype. Our data further emphasizes the utility of RNAi screens in identifying disease-associated genes.

Table of Contents

Chapter 1

Chapter 2

Chapter 3

Chapter 4

Chapter 5

List of Figures and Tables

List of Abbreviations

AONS – Anti–sense oligonucleotides

cDNA – Complementary DNA

ClC–1 – Chloride channel 1

CUBGP1 – CUG binding protein 1

DM1 – Myotonic Dystrophy Type 1

DM1 500 - Primary DM1 patient skin fibroblasts expressing ~500 CTG repeats

DM1 2000 - Primary DM1 patient skin fibroblasts expressing ~2000 CTG repeats

DMPK – Dystrophia Myotonica Protein Kinase

DMSO – Dimethyl sulfoxide

DNA – Deoxyribonucleic acid

ER – Endoplasmic reticulum

ERK – Extracellular signal–related kinase

FCS – Fetal calf serum

IC50– Half maximal inhibitory concentration

IR – Insulin receptor

MBNL1 – Muscle blind–like protein 1

mRNA – Messenger RNA

NHF - Normal human fibroblasts

PACT – Protein Activator of PKR

PBS – Phosphate buffered saline

PERK - protein kinase RNA-like endoplasmic reticulum kinase

PKC – Protein Kinase C

PKR - Interferon-induced, double-stranded RNA-activated protein kinase

PMSF – Phenylmethylsulfonyl fluoride

PRKRA - Protein kinase, interferon-inducible double stranded RNA dependent activator

qPCR – Quantitative polymerase chain reaction

RISC – RNA-induced silencing complex

RLC – RISC loading complex

RNA – Ribonucleic acid

SD – Standard deviation

SEM – Standard error of the mean

STDEV - Standard deviation of the mean

TAR – HIV-1 trans-activation response element

TRBP – TAR-RNA binding protein

ZNF9 – Zinc finger nine

Acknowledgements

I would like to sincerely thank my MSc thesis supervisor Dr. Alex MacKenzie for his unwavering support and guidance throughout the struggles and successes of my studies. His experience, rationale, and positivity provided a phenomenal learning experience for me, and is a man who I truly hold with the utmost respect. I would like to thank Dr. Stephen Baird for his help in developing the high-throughput screening platform and scanning my microscopy plates continually. I would also like to thank Dr. Faraz Farooq for his input at every stage of the project on experimental design and Dr. Francisco Molina for his technical expertise. I recognize Dr. Bob Korneluk for his pioneering work in the field of Myotonic Dystrophy that has made my work possible and for his input on my experiments. A special thanks as well to Fahad Shamim, Calvin Jary, and Nafisa Tasnim for their help during screen validation.

I would like to thank everyone at the Apoptosis Research Centre, especially Lynn Kelly, who make the whole facility run smoothly and contribute to a wonderful and engaging learning environment. I am very appreciative of my advisory committee members Dr. Alexandre Blais and Dr. Brian Foster for their guidance during the course of my time at the University of Ottawa.

Finally I would like to thank my wife Julianne, my personal and professional psychologist, for her support during my times of struggle in science.

Chapter 1

1. Introduction

1.1 Myotonic Dystrophy type 1 (DM1)

1.1.1 DM1 incidence and disease background

Myotonic dystrophy type 1 is the most common form of adult muscular dystrophy affecting approximately 1 in 8000 in the general population (Vignaud et al., 2010). The DM1 mutation is inherited in an autosomal dominant pattern and belongs to a class of more than 20 tri-nucleotide repeat expansion disorders (TREDs) (Brouwer et al., 2009). These disorders are all characterized by the pathogenic expansion of a trinucleotide motif within a gene. The location and extent of the expansion mutation within a particular gene impacts the specific manifestation of the disorder. Mutations in coding regions of a given gene result in gain of function toxicity as is seen in Huntingdon's disease, whereas mutations in non-coding regions can produce RNA gain of function toxicity, as is the case with DM1 (Galka-Marciniak et al., 2012).

There exists type 1 and type 2 myotonic dystrophy. Myotonic dystrophy type 1 (DM1) is caused by a CTG repeat expansion in the 3' untranslated region of the dystrophia myotonica protein kinase (DMPK) gene, which is found on chromosome 19 (Lee and Cooper, 2009). Myotonic dystrophy type 2 (DM2) results from a tetranucleotide repeat expansion of a CCTG motif found in intron 1 of the zinc finger nine (ZNF9) gene (Liquori et al., 2001). DM2 is more prevalent, does not manifest as a congenital or pediatric disorder, and is comparatively less debilitating (Amack et al., 2002; Suominen et al., 2011).

The mutation causing DM1 was first discovered in 1992 and shown to be a CTG repeat expansion in the 3' untranslated region of the DMPK gene (Hunter et al., 1992). It quickly became apparent that the length of the CTG repeat was proportional to the severity of the disease

(Brook et al., 1992; Harper, 2001; Hunter et al., 1992). The general population have repeat lengths in the range of 5-38 while mild symptoms begin to manifest in adulthood for individuals with expansions greater than 50 CTG repeats and a more severe congenital form of the disease has CTG repeat lengths as high as 4000 (Lee and Cooper, 2009). The repeats expansions are a result of an inherent genomic instability. Repetitive sequences are susceptible to slippage of the DNA replication complex during meiosis which causes the leading strand to be misread and the inclusion of extra bases (Liu et al., 2012). This phenomenon causes a trend of increasing length of CTG repeats through generations of affected families (Harley et al., 1992).

The nearly ubiquitous expression of DMPK means that a variety of tissues are affected in DM1, particularly those that are less mitotically active such as muscle and neurological tissues (Giagnacovo et al., 2012). DMPK RNA foci have been found to degrade during mitosis as more granules are pushed into the cytoplasm allowing this process to occur, while non-dividing cells are more susceptible to their accumulation (Giagnacovo et al., 2012). Disease manifestations include myotonia (inability to relax muscle after contraction), insulin resistance, cardiac defects (arrhythmias), testicular atrophy, cataracts, cognitive dysfunction, and muscle wasting (Lee and Cooper, 2009; Harper, 2001).

1.1.2 DM1 Molecular Pathology

The mapping of the DM1 CTG to a non-coding segment of the DMPK gene initially rendered the molecular pathogenesis obscure. Initial studies that demonstrated a decrease in the amount of functional DMPK protein produced in DM1 cells pointed to a mechanism of haploinsufficiency, where the loss of DMPK protein production from one allele was proposed to cause the disease (Fu et al., 1993). However, DMPK knocked out mice displayed neither DM1

associated myotonia, muscle wasting, nor a shortened lifespan, only a moderate atrioventricular conduction abnormality was observed (Berul, et al., 1999). A DMPK independent model was then hypothesized, in which expanded CTG repeats alone caused the disease. The identification of DM2 in 1998 pointed to an RNA gain of function mode of pathogenesis, since both diseases, which share clinical features were caused by repeat expansions in non-coding regions of different genes (Ranum et al., 1998). This theory was further supported by the production of mice expressing 250 CTG repeats in an α-actin gene that exhibited myotonia as well as the primary features of DM1 muscle histology: central nucleation of muscle fibers and the presence of ring fibers (Mankodi et al., 2000).

1.1.2.1 DMPK

DMPK protein function remains poorly understood but work done with a DMPK knockout mouse seems to indicate that it is a non-essential gene with only mild consequences for the mouse (Berul et al., 1999). Expression analysis of the DMPK transcript has detected mRNA in a variety of tissues (liver, skeletal muscle, heart, intestinal epithelium, bone, skin, lung, testis, smooth muscle, and brain) with the highest levels observed in heart tissue, skeletal muscle, and smooth muscle (Lam et al., 2000). DMPK is a serine/threonine kinase homologue of the p21-activated kinases MRCK and ROCK/rho-kinase/ROK (Kaliman and Llagostera, 2008). Several isoforms have been described although the roles of these different proteins is not precisely known. The C-terminal domain appears to affect the localization of the protein and perhaps substrate specificity. Isoforms A and B contain a hydrophobic C-terminus thought to confer localization to the endoplasmic reticulum whereas the hydrophilic C-terminus in isoforms C and D causes mitochondrial outer-membrane localization. E and F isoforms have a truncated C-

terminus and are cytosolic proteins (Kaliman and Llagostera, 2008; Wansink et al., 2003). Expression of DMPK protein is induced by the canonical myogenic pathway (p38 mitogenic-activated protein kinase, nuclear factor-B, phosphatidyl inositol 3-kinase) in *in vitro* models of mouse muscle, demonstrating a link between DMPK and muscle growth and regeneration (Kaliman and Llagostera, 2008; Carrasco et al., 2002). Ablation of DMPK interferes with the differentiation of myotubes through repression of MyoD and myogenin (Amack et al., 2002; Harmon et al., 2008) while DMPK overexpression interferes with C2C12 myoblast differentiation (Okoli et al., 1998). Myotubes lacking DMPK display a greater incidence of open voltage gated calcium and sodium channels, implying a role for DMPK in regulating fiber contractility (Benders et al., 1997; Lee et al., 2003; Mounsey et al., 2000).

As the role of haploinsufficiency of the DMPK protein in the development of DM1 has been precluded, the focus has shifted to an RNA mediated pathogenesis with a general consensus emerging that toxic gain of function of the DMPK transcript underlies DM1. However, in addition to putative toxic expanded DMPK mRNA, it is worth noting that the DMPK trinucleotide repeat results in hyper-condensation of chromatin around the DMPK locus and that the contiguous SIX5 demonstrates decreased transcriptional expression in DM1 cells (Otten and Tapscott, 1995). Potential repression of other genes may be an additional contributing factor as expanded mutant DMPK mRNA has been demonstrated to sequester transcription factors SP1 (specific protein 1) and STATs (signal transducers and activators of transcription) 1 and 3 (Ebralidze et al., 2004).

1.1.2.2 Nuclear Foci: MBNL1 loss of function

Despite the effects described in the latter section, the aggregation of expanded repeat DMPK mRNA into insoluble nuclear foci is increasingly attributed as the primary source of DM1 pathology (Davis, et al., 1997). Short segments of RNA containing CUG repeats have been shown to cause the formation of a hairpin loop structure due to C-G base pair binding (Napierala and Kryzosiak, 1997). The formation of DMPK nuclear aggregates containing such duplexes has been found to dysregulate the function of several RNA-binding proteins that are localized to the foci. A human homolog of the drosophila protein Muscle blind, Muscle blind-like protein 1 (MBNL1) was predicted to bind to the CUG hairpins (Miller et al., 2000) and was later indeed found to be sequestered to the RNA foci, thereby reducing its activity in the nucleus and cytoplasm (Jiang et al., 2004; Lin et al., 2006) while also preventing the nuclear export and degradation of DMPK mRNA (Smith et al., 2007).

Further studies with MBNL1 strengthened the argument for its role in the progression of DM1. MBNL1 -/- mice were generated that recapitulated the myotonia and cataracts seen in DM1 mice (Kanadia et al., 2003; Kanadia et al., 2006). MBNL1 has a key role in alternative splicing for a wide range of mRNAs, and its depletion from the nucleoplasm in DM1 by nuclear foci prevents proper processing of its target transcripts (Dansithong et al., 2005; Dansithong et al., 2008). DM1 is now understood to be a spliceopathy, in which over twenty mRNA transcripts normally regulated by MBNL1 are improperly processed (Ranum and Cooper, 2006). This includes the inclusion of fetal exons in its target transcripts, resulting in the expression of fetal isoforms of important proteins (Lee and Cooper, 2009). A number of these misregulated proteins are associated with a specific DM1 finding, such as myotonia with ClC-1 (chloride channel 1),

insulin resistance with IR (insulin receptor), and cardiac conduction defects with cTNT (cardiac troponin) (Mankodi et al., 2002; Kanadia et al., 2006; Ho et al., 2004).

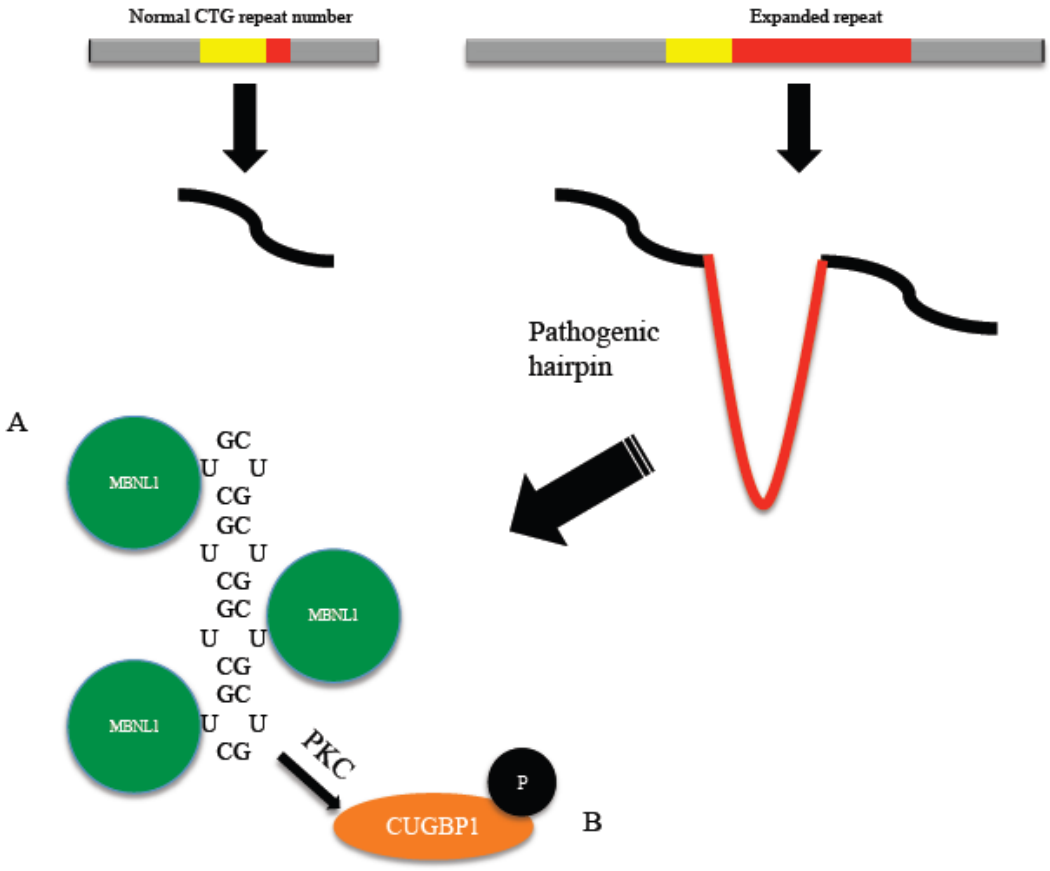

Figure 1: Mechanism of MBNL1 and CUGBP1 modulation by interaction expanded DMPK RNA.

A) The expanded region of DMPK RNA forms a secondary structure known as a hairpin loop which binds MBNL1, depleting it from the nucleoplasm. B) Activation of PKC pathway by an unknown mechanism leads to hyperphosphorylation and stabilization of CUGBP1. Misregulation of both MBNL1 and CUGBP1 lead to switch in alternative splicing programs, changing the expression of several transcripts.

1.1.2.3 Nuclear Foci: CUGBP1 gain of function

CUG binding protein 1 (CUGBP1) has also been identified as a second RNA binding protein that is misregulated in DM1. As suggested (incorrectly) by its name, CUGBP1 was initially characterized as a protein that binds CUG rich single stranded RNAs. However, it does not interact directly with DMPK CUG hairpin loops or localize to DM1 nuclear foci (Mankodi et al., 2003; Fardaei et al., 2002; Timchenko et al., 1996). In contrast to MBNL1, CUGBP1 demonstrates a gain of function by increased stabilization in DM1 cells promoting the inclusion of fetal exons in ClC-1, cTNT, and IR (Philips et al., 1998; Savkur et al., 2001), further exacerbating the spliceopathy. CUGBP1 has also been identified as a regulator of mRNA decay in muscle cells *in vitro* by destabilization of target transcripts (Lee et al., 2010) and it has been found to preferentially bind to 3'UTR to initiate mRNA decay (Masuda et al., 2012). It appears that CUGBP1 and MBNL1 act in opposing fashion with the former acting during fetal and the latter in adult development, promoting the expression of different isoforms of many genes. This is supported by their expression patterns; CUGBP1 is highly expressed in fetal tissue during embryogenesis while MBNL1 expression is repressed. The pattern switches during adulthood, where MBNL1 expression is enhanced and CUGBP1 expression is repressed (Lin et al., 2006; Kalsotra et al., 2008).

While the loss of function of MBNL1 in DM1 is well determined by its sequestration in nuclear foci, the mechanism of enhanced expression of CUGBP1 is poorly understood. Stabilization of CUGBP1 protein has been observed by its hyperphosphorylation of target sites by Protein Kinase C isoform α (PKCα) (Kalsotra et al., 2008; Kuyumcu-Martinez et al., 2007; Lee and Cooper, 2009). The expanded DMPK CUG mRNA mediated activation of PKCα has not been explained to date. Over-expression of CUGBP1 in animal models recapitulates some of

the features of DM1, namely cardiomyopathy, cardiac conduction defects, and decreased lifespan (Koshelev et al., 2010; Wang et al., 2007; Ward et al., 2010). A direct role of PKCα activation on DM1 progression is further supported by the amelioration of the cardiac defects in mice administered a PKCα inhibitor (Wang et al., 2009). Of the two pathogenic mechanisms, the MBNL1 deficit is believed to exert a greater pathogenic effect.

1.1.2.4 Endoplasmic Reticulum Stress

While much of the DM1 pathology is a result of DMPK nuclear foci and resultant transcript missplicing, the precise source of muscle wasting and atrophy has not been attributable to any one cause. In addition to the observed aberrant splicing of extracellular matrix genes there has been some evidence of endoplasmic reticulum (ER) stress as the source of muscle degeneration (Du et al., 2010). ER-stresses may be initiated by accumulation of unfolded proteins, alterations in Ca2+ homeostasis, and decreased protein glycosylation, that all may lead to apoptosis. Specifically, the missplicing of ryanodine receptor (RyR1) and Sarcoplasmic/endoplasmic reticulum Ca2+ ATPase (SERCA) in DM1 has been shown to deregulate Ca2+ homeostasis and initiate ER stress in DM1 tissues (Kimura et al., 2005; Ikezoe et al., 2007). Muscle biopsies of DM1 patients, reveal sign of ER stress including increased expression of GRP78 and calnexin, and increased phosphorylation of PERK and eIF2α in fibres displaying sarcoplasmic masses and pyknotic nuclei (Ikezoe et al., 2007). These are all factors involved in ER-stress mediated apoptosis, which may play a role in the degeneration of DM1 muscle tissues.

1.1.3 DM1 Therapeutics

Therapeutics strategies for the management of DM1 have, to date, concentrated on symptom management with the use of sodium channel blockers such as mexiletine to alleviate myotonia (Wheeler et al., 2008). A few ongoing clinical trials have attempted to treat the source of the disease but have been as yet unsuccessful (Wheeler et al., 2009).

1.1.3.1 Gene Therapy

The identification of the role of toxic RNA in the aggregation of MBNL1 and its role in the regulation of alternative splicing has highlighted the potential of RNA foci as a therapeutic target in DM1. Translational research for DM1 is often aimed at the disruption of the interaction between MBNL1 and the expanded repeat hairpin RNA, elsewhere there are attempts to selectively degrade mutant DMPK, or to suppress DMPK expression altogether (Mulders et al., 2010).

Hammerhead ribozymes directed against DMPK transcripts show some potency in lowering the number of RNA foci and partial correction of splicing abnormalities *in vitro,* though problems containing the effect to the nucleus resulted in overall depleted DMPK (Langlois, 2003). Another anti-sense oligonucleotide (AON) strategy has been successful in reducing foci formation and correcting some splicing defects in vivo through direct recruitment of RNAse H to DMPK mRNA, though no impact was seen on myotonia (Mulders et al., 2010). AONs specifically targeting the mutant DMPK over the wild type have reduced mutant transcripts by 80%, though delivery and specificity in these experiments were poor, presumably due to the inaccessibility of the pre-mRNA target sequences (Furling et al., 2003). Pre-clinical

use of siRNA against DMPK has also been attempted, although targeting the nucleus has proven problematic (Magana and Cisneros, 2011).

Although many promising approaches to DM1 treatment are under development, much work remains to further validate these molecules, particularly AONs, with respect to their absorption and metabolism before they reach patients.

1.1.3.2 MBNL1

A number of small molecules have been shown to inhibit MBNL1 binding to the expanded CUG tract of DMPK and attenuated splicing defects in culture. One example is pentamidine, which is proposed to free MBNL1 from RNA foci by binding to DMPK expanded transcripts, thereby reducing the splicing abnormalities observed in a HeLa model expressing expanded CUG RNA (Warf et al., 2009). The high toxicity of this compound limited its in vivo suitability, but its capacity to improve missplicing serves as an encouraging proof of principle, prompting further chemical screens for small molecules with high affinity for the CUG hairpin loop. Garcia-Lopez and colleagues have identified a small peptide capable of preventing CUG-RNA hairpin formation, which has shown some promise in mice by reversing RNA toxicity (2011). Overexpression of MBNL1 has also been highlighted as a promising strategy. In the murine and *Drosophila* model of DM1, HSA^{LR}, overexpression of MBNL1 has been effective in rescuing the splicing patterns of ClC-1 and IR, resulting in the reduction of myotonia observed in the mice (Kanadia et al., 2006; De Haro et al., 2006). It has more recently been shown as well that MBNL1 long-term overexpression prevents myotonia, splicing defects, and myopathy in DM1 mice (Chamberlain and Ranum, 2012).

1.1.3.3 CUGBP1

Further attempts to treat involve the reduction in CUGBP1 activity to correct missplicing. The foci conferred activation of PKCα, by an as yet unknown mechanism, stabilizes CUGBP1and some success has been achieved in a transgenic CUGBP1 over-expressing mouse model using a selective PKC inhibitor, with a decrease in CUGBP1 levels, improved splicing of cardiac troponin, and decreased cardiac arrhythmia (Wang et al., 2009). Studies such as this point to CUGBP1 modulation as another viable treatment strategy.

1.1.3.4 Splicing Rescue

Treatment approaches that circumvent the primary DM1pathogenic foci and target further downstream have been attempted such as modifying the transcriptome using AONs. These oligonucleotides can be designed to bind premRNA splice sites and promote the exclusion of fetal exons (Magana and Cisneros, 2011). The most successful example to date has been an AON that prevents the inclusion of exon7a into ClC-1, which itself contains a stop codon that prevents expression of the full length chloride channel. By blocking the inclusion of this exon, increased functional levels of ClC-1 protein can be attained, reducing myotonia in a CTG-overexpressing mouse model of DM1 (Wheeler and Thornton, 2007).

1.1.3.5 Future Directions

Symptom management is the only type of therapy currently in use for DM1 patients, specifically the management of myotonia with sodium channel blockers (Logigan at al., 2010). While many approaches are getting closer to providing clinical value, there are none currently available to patients.

1.2 High-Throughput RNAi Screening

Advances in sequencing and genomics in recent years have aided in the compilation of whole genome RNA interference (RNAi) libraries for many model organisms. Using platforms similar to those used for large scale chemical screening, high-throughput RNAi screens mimicking single gene knockouts are now feasible (Boutros and Ahringer, 2008).

Many different types of RNAi libraries are now available for organisms, with different suitability for different screens. Small interfering RNA (siRNA) remains the cheapest and simplest means, but relies on lipid vectors for cell entry and can have very variable efficacy depending on the cell type being used. Lentiviral packaged short-hairpin RNA (shRNA) provide more sustainable and less variable gene knockdowns due to their genomic integration in the host cell but are more costly (Boutros and Ahringer, 2008).

Three measures of data quality are typically used to assess the efficacy of high-throughput screens. Signal to noise ratio (SNR) indicates the difference between an output measure in a positive cell line and a negative cell line (Birmingham et al, 2009). For example, when using a fluorescent output for screening, the SNR would be calculated between a cell exhibiting the fluorescent trait and one that is not. In the case of DM1 fibroblasts used in this screen, the SNR would be calculated on the fluorescent signal between a DM1 fibroblast and a normal fibroblast, to determine how much of the signal is attributable to non-specific background fluorescence. The coefficient of variation is used as a measure of the data spread amongst the sample population, given that the majority of samples should have no effect on cells (Birmingham et al., 2009). Lastly, the Z'-factor is used as a measure of the feasibility of a screen based on the separation between positive controls and untreated controls (Birmingham et al.,

2009). This is defined numerically as Z' = 1- (3SD of samples + 3SD of controls)/(| Mean of samples - Mean of controls |) and gives an indication of how easy it will be to identify hits and whether there is overlap in the ranges of positive and untreated controls (The samples in this case are DM1 cells treated with MBNL1 siRNA, and controls are DM1 cells treated with non-targeting siRNA).

Values for the Z'-factor < 0 indicate an overlap in the ranges of samples and positive controls, meaning it is unlikely to be easy to discern hits. Where $0 < Z' < 0.5$ indicate a good separation between controls, indicated a feasible screen. A $Z' > 0.5$ indicates an excellent separation and robust screening assay conditions (Birmingham et al., 2009).

Though based on similar platforms, there remain important differences in the setup and data analysis of RNAi and small-molecules screens. Comparisons of 19 optimized siRNA screen and 13 small molecule screens performed at ICCB-Longwood Screening Facility (Harvard Medical School) found that the cross-plate data was more normally distributed amongst the RNAi screens (Birmingham et al., 2009). In comparison to chemical screens, RNAi screens displayed SNRs 50% lower, coefficients of variation twice as high, and lower Z'-factors (typically between 0 and 0.5) (Birmingham et al., 2009). It is thus clear that siRNA screens generally demonstrate less robust data than chemical screens. These differences can be primarily attributed to the nature of RNA interference. The compilation of siRNA library involves the amalgamation of hundreds or thousands of gene directed oligonucleotides. Every one of those siRNAs has a predicted or validated gene knockdown, meaning that each sample should have some cellular effect that could indirectly modify the screening phenotype (Perrimon and Mathey-Prevot, 2007). This can lead to larger variation in the sample population. The opposite is true for the large majority of compounds in a chemical library that may have no biological activity. Gene

knockdown in RNAi experiments occur at different times based on the half-life of the target protein and the efficiency of the siRNA. Assays typically occur over 48-72hrs whereas chemical screens can be done over a few hours. The increased time of cell culture can introduce environmental variation and impact the assay. RNAi is susceptible to false-negatives if a gene is not knocked down by the assay end-point and false-positives can appear due to downstream or off-target effects (Perrimon and Mathey-Prevot, 2007). Delivery of the siRNA molecules can also introduce variation in a screen. Transfection with lipid reagents may have variable efficiency of delivery and may cause stress that is sufficient to impact cellular phenotypes (Birmingham et al., 2009). The same is true with control selection. No truly negative control is available for siRNAs. A non-targeting sequence is generally used but they may still produce off target effects (Birmingham et al., 2006). Positive controls also display more variability because of transfection efficiency and generally are less effective than in chemical screens (Birmingham et al, 2006).

While genetic screens have great potential for the discovery of new biological interactions, there remain difficulties in hit selection due to the possibility of false-positive and false-negative results. A study investigating the consistency of normalization procedures for a high-throughput *Drosophila* RNAi screen, which tested the rate of validation of hits in secondary screening, found that no method amongst seven tested performed better than the others (Wiles et al., 2008). Hit selection that is too rigorous has the potential to miss transient and variable, though valuable, hits, while looser selection parameters may include too many false positives (Birmingham et al, 2009). Statistical parameters used for normalization and hit selection are varied and each have their benefits. The Z-score is used to rank samples based on the number of standard deviations from the sample mean (mean +/- k standard deviations) that is easy to

calculate and visualize. An improvement on this calculation is the robust Z-score that uses the median absolute deviation to score samples (median +/- k median absolute deviations). This technique can identify weaker hits than the regular Z-score and is less sensitive to outliers (Birmingham et al., 2009). In this regard it is worth noting that PACT may not have been identified exclusively using stringent Z-score criteria.

Thus, although high-throughput RNAi is an increasingly important tool for biological loss-of-function discoveries, it nonetheless involves many challenges for the identification of these interactions. Statistical techniques inevitably carry with them assumptions and limitations that must be brought into consideration. It is important to note that thorough secondary screening is a necessity when considering the outcomes of RNAi screens, to ensure the validity of any identified hits, as even the most advanced statistics are unable to conclusively confirm primary hits.

High-content cellular assays using fluorescent outputs have enormous potential for the understanding of disease specific biology. Cellular features specific to disease states may be difficult to analyze and find appropriate controls for. The expression of nuclear foci in DM1 cells and their short half-life make them a perfect candidate for genetic screening.

1.3 PRKRA (PACT)

PRKRA, or PACT, was one of the top hits in our kinome RNAi screen for foci modulating genes in DM1 cells and was therefore of interest for further study. PACT is a kinase involved in stress response that can interact with double-stranded RNAs (dsRNA)(Singh and Patel, 2012). PACT is a pro-apoptotic factor that activates protein kinase R (PKR). PKR has been found to be over-expressed in DM1 cells which makes PACT a good candidate for involvement in DM1 foci (Mankodi, et al., 2003). PKR knockout mice have been bred with a DM1 model to create PKR knockout DM1 mice. However, no significant impact on disease progression were reported (Mankodi et al., 2003). PACT (PKR ACTivator) exists in complex with another RNA-binding protein, TAR-RNA binding protein (TRBP); the two proteins exert opposing effects on PKR activation. During cellular stress, PACT dissociates from TRBP, homo-dimerizes, and phosphorylates PKR (Singh and Patel, 2012). Active PKR then phosphorylates eIF2α, inhibiting the formation of the translation initiation complex and halting global protein synthesis (Singh and Patel, 2012). PACT is normally inhibited from activating PKR by binding to TRBP (Singh and Patel, 2012). TRBP and PACT are also involved in the RNA interference pathway, forming a complex with DICER (Daniels and Gatignol, 2012).

A potential connection for PKR and PACT to DM1 muscle wasting is supported by the involvement of both proteins in the ER-stress response and the presence of ER stress mediated apoptosis in DM1 (Ikezoe et al., 2007). PACT has been shown to be necessary for tunicamycin induced apoptosis through ER stress. Tunicamycin prevents protein glycosylation which induces ER stress and apoptosis. Singh et al. (2009) found that PACT undergoes phosphorylation following tunicamycin treatment and that PACT-induced PKR activation is essential for the induction of apoptosis. It was also shown that PACT and PKR null cells are

resistant to tunicamycin induced apoptosis, that they rescue the phenotype upon their addition (Singh et al., 2009) and that this process is independent of the protein kinase RNA-like endoplasmic reticulum kinase (PERK) (Lee et al., 2007). In addition, PKR has been found to directly activated by CUG repeats in DM1 and activate the p-eIF2α pathway, inhibiting translation of several mRNAs, which may also lead to progressive muscle loss (Huichalaf et al., 2010).

PACT also plays a role in RNA interference processing through Dicer. RNA interference involves the cleavage of short RNA fragments by Dicer to create microRNA (miRNA) and short interfering RNA molecules (siRNA) which reduce the expression of their target mRNAs. RNAi is a highly conserved post-transcriptional mechanism for knocking down gene expression. Dicer is the main endonuclease involved in the pathway, binding to Argonaute (Ago), and either TAR-RNA binding protein (TRBP) or PACT to form the RNA-induced silencing complex (RISC) loading complex (RLC) (Takahashi et al., 2013). Dicer has the ability to associate with both PACT and TRBP which produce distinct modes of processing for double-stranded RNAs (dsRNA) (Lee, et al., 2013). PACT in complex with Dicer has been shown to inhibit loading of pre-siRNA molecules in contrast to Dicer alone and TRBP-Dicer, demonstrating a role for these two double-stranded RNA-binding proteins (dsRBPs) in substrate and cleavage specificity (Lee et al., 2013). Takahashi and colleagues (2013) have also shown that both monomeric TRBP and PACT has greater affinity for siRNA than the homo-dimeric forms of both proteins. Targeting of mRNAs by miRNA is also enhanced for complexes containing PACT but not for TRBP (Noland and Doudna, 2013). Alterations in miRNA expression have been found in Drosophila expressing expanded CTG repeats and are conserved in DM1 patient biopsies (Fernandez-Costa et al., 2012). Taken together, TRBP and PACT both affect the expression of fundamental genetic

pathways through their differences in affinity for siRNA and miRNA; if aberrant miRNA expression underlies some aspects of DM1 pathology there may be some therapeutic value in its correction.

1.4 Hypothesis and Objectives

A high-throughput RNAi screen against protein kinases in DM1 primary cells will identify modifiers of DM1 nuclear DMPK mRNA foci size and number. Our objectives are to identify foci-modifying genes, confirm their impact on DMPK mRNA foci which is a key DM1 biomarker and, if possible, identify the mechanism of this action.

1.5 Project Rationale

It is clear that DMPK mRNA foci are a primary source of DM1 pathology and the disruption of these foci may be of significant clinical importance. An effective Myotonic Dystrophy type 1 therapeutic may also target the stress caused by the expression of expanded repeat DMPK RNA. In order to develop such directed therapeutics for DM1, a more thorough understanding of the dynamics of CUG RNA foci is necessary.

With an aim to understand foci dynamics and identify genetic factors that affect their aggregation, as well as identify potential therapeutic targets, a high-throughput Kinome RNAi screen was performed in DM1 patient fibroblasts. As kinases represent critical control points in cellular signaling and are perceived to be highly druggable, the entire set of human protein

kinases has been the subject of drug discovery queries and genomics in recent years and we believed represented an appropriate subset for therapeutic target discovery for DM1.

A short list of leads was compiled of kinases which when inhibited, decreased the size and number of nuclear RNA foci. Secondary validation of primary leads from the screen identified PACT as a novel genetic modifier of DM1 nuclear foci. Given the role of PACT in the activation of PKR, and the previous implication of PKR in the activation of apoptosis in DM1, PACT was an ideal candidate for further evaluation. PACT knock down by siRNA decreases the size and number of DM1 RNA foci and effects the expression of MBNL1 and CUGBP1 proteins. The resultant modification of these key DM1 splicing factors causes an increase in the inclusion of exon 11 in the insulin receptor transcript.

We found that inhibition of PKR with a small molecule also results in a decrease in the expression of foci but does not induce MBNL1 protein. This confirms previous studies findings of PKR over-activation in DM1 cells (Huichalaf et al., 2010) and highlights PKR's potential as a therapeutic target. In addition, the knockdown of PACT in control human fibroblasts (non-DM1) also stimulates the expression of MBNL1, implying that induction of MBNL1 by PACT siRNA treatment is a not dependent on the presence of nuclear foci.

Further probing of PACT interacting proteins demonstrated that the knockdown of TRBP protein with siRNA also stimulates expression of MBNL1 and improves splicing patterns of ClC-1 and IR, with a more modest effect on foci reduction than PACT. Given the antagonistic properties of TRBP and PACT on PKR activation it is not intuitive that their knockdown by siRNA would have a similar effect on foci or MBNL1 expression.

Chapter 2

2. Methods

2.1 High-Throughput Screening

2.1.1 Transfection

Cells were transfected with siRNA using Lipofectamine RNAi MAX lipid reagent at a concentration of 0.08uL per well in a 384-well plate. Reverse transfection was performed by spotting 5uL of 8x siRNA (80nM) in water then spotting 5uL of OPTIMEM containing 0.08uL of Lipofectamine RNAi MAX to each well, then incubating at room temperature for a minimum of 20 minutes to allow integration of siRNA molecules into lipid micelles. The cells were then washed with PBS and trypsin was added to dislodge cells from the tissue culture plate. Cells were then pelleted by centrifugation at 300g for 15 minutes to remove trypsin from the media. The pellet was then re-suspended in antibiotic-free DMEM-High Glucose and counted using a haemocytometer. Cells were then seeded at 800 cells in 30uL media (final well volume 40uL), and incubated at 37C and 5%CO2 for 96hrs. All reagents were added using the Biotek Multidrop Cell Dispenser. Falcon 384-well plates were used for tissue culture. Transfection efficiency was assessed by 20nM ALL-STAR Death Control siRNA (Invitrogen). This siRNA targets several common sequences in essential ubiquitin genes and the Alu family. The depletion of these genes results in apoptosis, the degree of apoptosis observed thus giving a readout of transfection efficiency.

2.1.2 Fluorescence in situ Hybridization

Following the incubation period, cells were fixed by adding 40uL of 8% formaldehyde in each well for 10 minutes, for a final concentration of 4% formaldehyde. The plates were then emptied using the plate aspirator and washed using 80uL of 1x DPBS. The cells were then permeabilized by adding 50uL of 70% ethanol to each well and incubating at 4C overnight. The plates were then washed twice with 50uL of 1xDPBS. The hybridization was performed by adding 30uL of 0.1ng/uL AlexaFluor555nm-(CAG)10 probe in DIG Easy Hyb Granules Buffer. The plates were then incubated at 37C for 2hrs. The plates were then washed three times with 1xDPBS for 5 minutes each. Nuclei were then stained by adding 30uL of 5ug/mL Hoechst stain in PBS for 10 minutes. The plates were washed once more with 1xDPBS for 5 minutes and then stored with 50uL of 1xDPBS. Plates were sealed with clear plastic plate covers to prevent dehydration.

2.1.3 High Content Image Analysis

Plates were scanned using the automated Opera High-Throughput Fluorescent Microscope. 15 images were captured for each well in order to include as many cells as possible in the quantification of nuclear foci. Images were uploaded to Columbus software where the RNA-foci were quantified in each cell. Cells were scored on the number of foci detected per nuclei and on the surface area of each foci as determined by the number of pixels covered in each foci. A minimum surface area threshold was included as the lower end of detection to ensure that background signal was not included in quantification. The Z-score was then used to rank samples based on the number of standard deviation from the mean. Samples that had a mean z-score from

three repeats less than -2.00 in either foci number per nuclei or mean foci surface area were considered hits and were further validated. Samples having a z-score greater than 2.00 were not included as hits as lethal siRNAs were more susceptible to outliers in this direction.

2.2 Western Blots

Cells were washed twice with Phospho-buffered saline (1 x PBS) and lysed with 175uL of RIPA buffer containing 10mg/ml each of aprotinin, phenylmethylsulfonyl fluoride (PMSF) and leupeptin for 30 min at 4°C. Following lysis, the samples were centrifuged at 13,000g for 20 minutes at 4°C and supernatants were collected and frozen at -20°C. Protein concentrations were determined by Bradford protein assay using a Bio-Rad protein assay kit (Richmond, CA, USA). Before analysis, samples were boiled for 5 mins and equal amount of protein extracts were separated by 11% SDS-Page (80 volts 30min, 120V, 1 hour). Proteins were subsequently transferred (30V, 12hrs) to nitrocellulose membrane and the membrane was incubated in blocking solution (PBS-T, 5% milk) for 1h at room temperature followed by overnight incubation with the primary antibody. Primary antibodies were purchased from Abcam and used as such: MBNL1-mouse IgG (1:5000), Tubulin-mouse IgG (1:20000), PACT-rabbit IgG (1:2000), TRBP-rabbit IgG (1:2000). Membranes were washed with PBS-T (1x PBS, 0.2% Tween-20) three times followed by incubation with HRP-liked secondary antibody (anti-mouse at 1:5000 and anti-rabbit at 1:2000) for 1 hour at room temperature. Secondary antibodies were purchased from Cell Signaling Technologies. Antibody complexes were visualized by autoradiography using ECL western blotting system (GE Healthcare) and X-Ray film (Kodak).

Quantification was performed by scanning the autoradiographs and signal intensities were determined by densitometry using Image J software.

2.3 RT-PCR Analysis

Total RNA was isolated according to the protocol provided by the manufacturer using the RNeasy 96-well extraction kit. Isolated RNA was treated with DNase to remove genomic DNA contamination. For qPCR, cDNA was reverse transcribed from isolated RNA employing the provided primer mix (oligodT primers/random primers) provided with the Quantitect Reverse Transcription kit (Qiagen). cDNA synthesis was conducted following manufacturer's instructions. Samples were normalized by quantification of DNA concentration using the NanoDrop Spectrophotometer. PCR was then performed on the isolated cDNA to assess splicing changes in genes affected by DM1 (ClC-1, IR). Primer sets for B-2-microglobulin, PACT, and TRBP were obtained from Origene. Primer sequences for ClC-1 and IR were taken from the literature so that the primer sets bind on either side of an exon. Multiple bands then occur based on the transcript variants that include or exclude that exon. β-2-microglobulin and GAPDH were chosen as housekeeping genes. Standard curves were generated for each primer pair to ensure our amplification and detection were occurring efficiently and within the linear range. The following primer sequences were used:

DMPK

Forward	5'-AGCCTGAGCCGGGAGATG-3'
Reverse	5'-GCGTAGTTGACTGGCGAAGTT-3'
Product Length:	63 bp

GAPDH

Forward	5’-TGAAGGTCGGAGTCAACGGATTTGG-3’
Reverse	5’-GGAGGCCATGTGGGCCATGAG-3'
Product Length:	989 bp

Insulin Receptor

Forward	5’-CCAAAGACAGACTCTCAGATCC-3’
Reverse	5’-ACATTCCCAACATCGCCAAGGG-3’
Product Length:	IR A (-exon 11) 137 bp
	IR B (+exon 11) 173 bp

β-2-microglobulin

Forward	5'-CCACTGAAAAAGATGAGTATGCCT-3'
Reverse	5'-CCAATCCAAATGCGGCATCTTCA-3'
Product Length	126 bp

PACT

Forward	5'-CCCTTAATGCCTGACCCTTCCA-3'
Reverse	5'- CAGGAAGTCTCCAGCCATGATG-3'
Product Length:	97 bp

TRBP

Forward	5'-AAGACGCCTGTGTACGACCTTC-3'
Reverse	5'- TTGTGCTTGGCTGCCTTCTTGC-3'
Product Length	128 bp

2.4 Cell Culture

DM1 $(CTG)_{500}$ patient fibroblasts, DM1 $(CTG)_{2000}$ patient fibroblasts, and Normal human fibroblasts (NHF) were cultured under standard conditions on 25 cm plates (Cell Star, Greiner Bio One) and kept at 37°C in a water-saturated environment which contained 5% C02. Dulbecco's modified Eagle's medium supplemented with 10% fetal calf serum (FCS) and 100 units/ml of penicillin-streptomycin was used as growth media. All growth plates were carefully monitored and were split when cells reached 70% confluence.

2.5 Statistical Analysis

For statistical analysis of transcript/protein increases or decreases, the students t-test (2 tailed, two-sample unequal variance test) was used. All graph error bars represent the standard error of the mean (SEM) as outlined in the figure caption.

Chapter 3

3. Results

3.1 High-throughput Screening

3.1.1 Assessment of DM1 cellular phenotype for screening

Myotonic dystrophy type 1 cell lines were assessed for their suitability for use in high content image acquisition and quantification of nuclear RNA-foci (Figure 2). The expression of nuclear foci in the DM1 primary skin fibroblast cell line expressing 500 CTG repeats in the DMPK gene (DM1 500 from here forward) tagged with a CAG-fluorescent probe provides a strong distinct signal that is not readily detectable in the normal human fibroblast cell line (referred to as NHF hereafter). The background fluorescent signal provided by the probe in NHF cells is below the threshold of detection used in quantification. This results in no detectable foci, and therefore a high signal to noise ratio (SNR) is present (Figure 3).

Quantification of nuclear foci in cell lines with increasing numbers of CTG repeats (Figure 3) reveals in general a varying expression of nuclear foci. DM1 2000 cells express more nuclear foci than DM1 500 cells, consistent with their validity as a biomarker of DM1 disease severity.

DM1 500 cells were selected for screening due to their ease of growth, the strength of the expression of nuclear foci, and their ease of transfection. Transfection efficiency was calculated using ALLSTAR Death siRNA, where the knockdown of several genes induces apoptosis. The percentage of cells lost then compared to controls gives an estimation of transfection efficiency. The DM1 500 cell line displays approximately 80% transfection efficiency after 96hrs of incubation with ALLSTAR Death siRNA (Figure4). This is comparatively less efficient than the

transfection observed for NHF cells, but was deemed sufficient for the purposes of genetic screening. The assumption of sufficient transfection efficiency was confirmed during the siRNA knockdown of our positive control MBNL (chosen for its role in foci formation). Treatment of DM1 500 cells with siRNA against MBNL1 resulted in an efficient knockdown of the protein over 96 hrs and a resultant decrease in the expression of nuclear foci (Figures 5 and 6). The absence of MBNL1 following siRNA treatment prevents the sequestration of expanded CUG hairpins into nuclear foci. Comparison between positive and negative controls gave a Z'-factor of 0.5, reflecting both the robustness of the assay and appropriate nature of the control. The screen was performed in triplicate and cells were fixed after 96hrs of incubation with siRNAs.

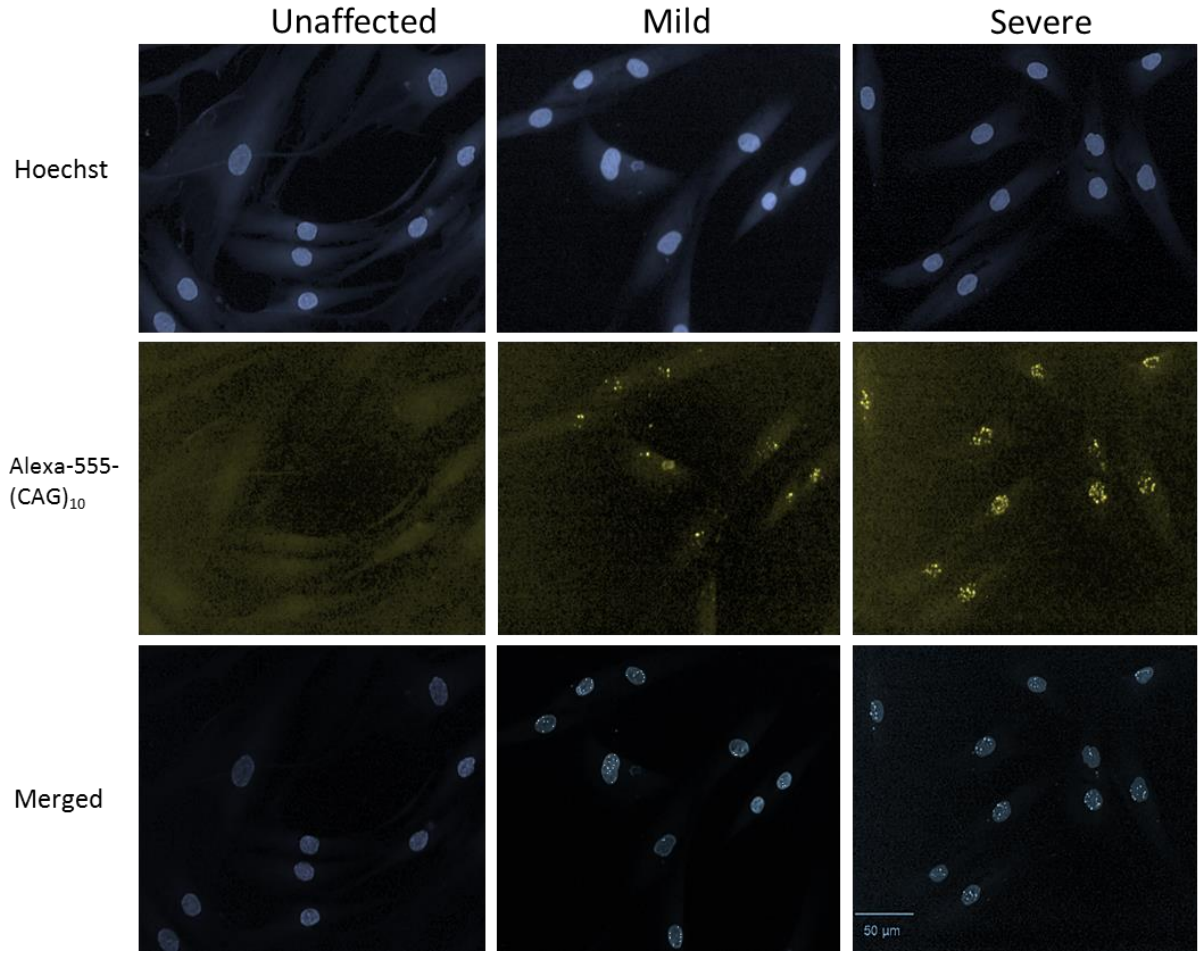

Figure 2: Myotonic Dystrophy type 1 cell lines express different numbers of nuclear RNA foci: Nuclear foci may be visualized by hybridization with fluorescently tagged (Alexafluor555)-CAG_{10} oligonucleotide probe. The wild type cell does not display any detectable foci (<50 CTGs), while mildly affected DM1 fibroblast display a moderate number of foci (~500 CTGs), and more severely affected DM1 fibroblast display a large number of foci (~2000 CTGs).

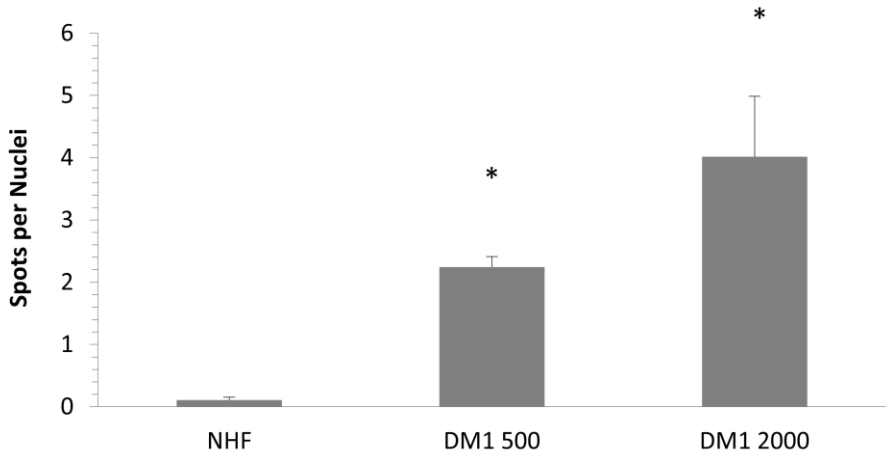

Figure 3: In Situ Hybridization assay for nuclear foci can detect significant differences in foci numbers per nuclei between cell lines: Fluorescence in situ hybridization assay of ALEXA555-$(CAG)_{10}$ targeted to the expanded DMPK mRNA CUG repeat in cell lines with increasing numbers of CTG repeats reveals increasing foci count (* DM1 500 significantly different from NHF, * DM1 2000 significantly different from DM1 500 (* $p<0.05$)).

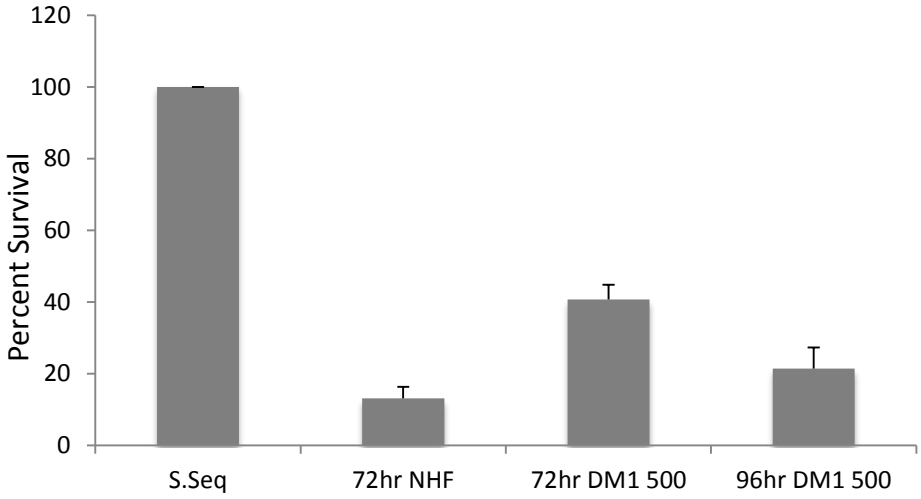

Figure 4: DM1 Fibroblast $(CTG)_{500}$ demonstrate high rate cell death after transfection with ALLSTAR Death siRNA control: ALLSTAR Death siRNA control incubated for 96hrs in DM1 500 fibroblasts demonstrate nearly 80% transfection rate compared to control (scrambled sequence(S.seq))siRNA treated cells. Normal human fibroblasts (NHF) demonstrate a higher degree of transfection that DM1 500 fibroblasts after 72hrs. (n=3)

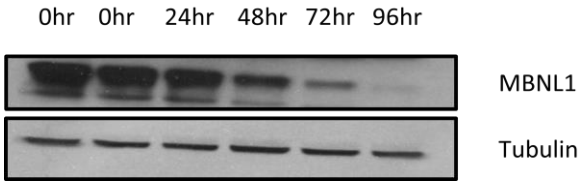

Figure 5: DM1 Fibroblast $(CTG)_{500}$ treatment with siMBNL1 (10nM) reduces MBNL1 protein expression over 96hrs.

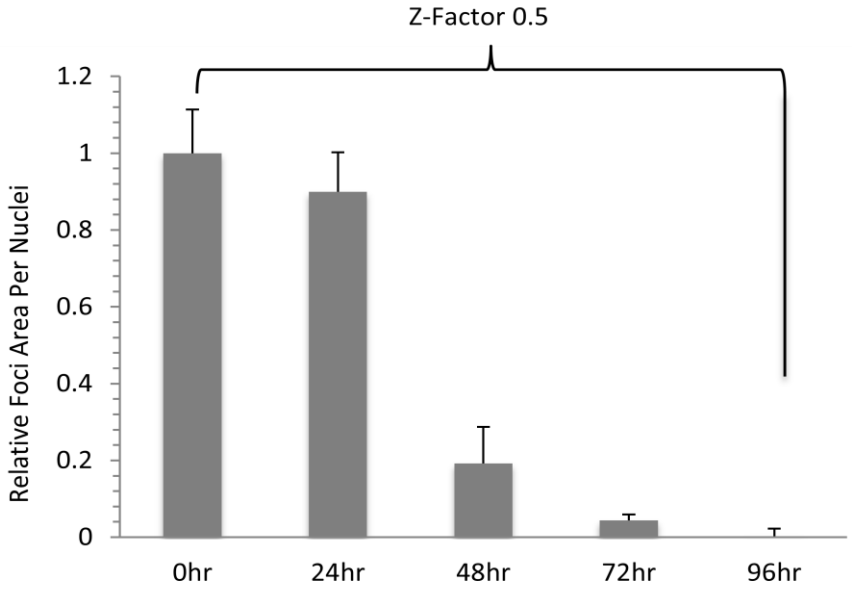

Figure 6: Knockdown of MBNL1 protein reduces nuclear foci: Treatment of DM1 500 fibroblasts with siMBNL1 at 10nM reduces the surface area of foci to below the threshold of detection over 96hrs. (error bars indicate st dev for n=3)

3.1.2 Screening Data

DM1 fibroblast cell cultures were incubated with individual siRNA's targeted against each of 518 kinases, the foci number and size (surface area) were quantified and normalized to facilitate comparison. The sample size was reduced by eliminating siRNA that upon initial analysis appeared cytotoxic and for which the reliable observation of normal foci expression would be impossible. Lethal siRNAs were defined as those demonstrating a Z-score of less than -2.0 for nuclei count, that is, samples whose cell count was less than two standard deviations below the mean. The raw data for one of the plates is shown in Figure 7. There is a strong separation between foci metrics conferred by positive control and those resulting from the sample group. Interestingly, the non-targeting siRNA used as a negative control appears to result in foci that are slightly more numerous and larger than those resulting from most kinases. The exact reason for this is unclear; it appears that RNAi modulation of most kinases appear to slightly reduce foci number and size, although the underlying biological mechanism and precise implications if this is true are unclear. In any event, we are most interested in those kinases with the most profound impact on the foci.

The remaining data set was normalized using the Z-score to quantify the number of foci observed per nuclei, as well as the mean surface area occupied by foci per nucleus (pixels squared). This measure uses the kinase RNAi sample mean rather than the negative control (non-targeting siRNA) to calculate variance. The normalized cross-plate data is compiled in Figure 8. Hits were then selected based upon mean Z-score values across the three replicates less than -2.0 in either category, indicating kinases that, when inhibited, may reduce the formation of nuclear foci. A short list of potential hits is outlined in Table 1.

Few kinases met our criteria of a mean Z-score below -2.0 for either foci number or foci area. PACT was only kinase to demonstrate Z-scores below -2.0 for both categories tested and was therefore selected for further validation.

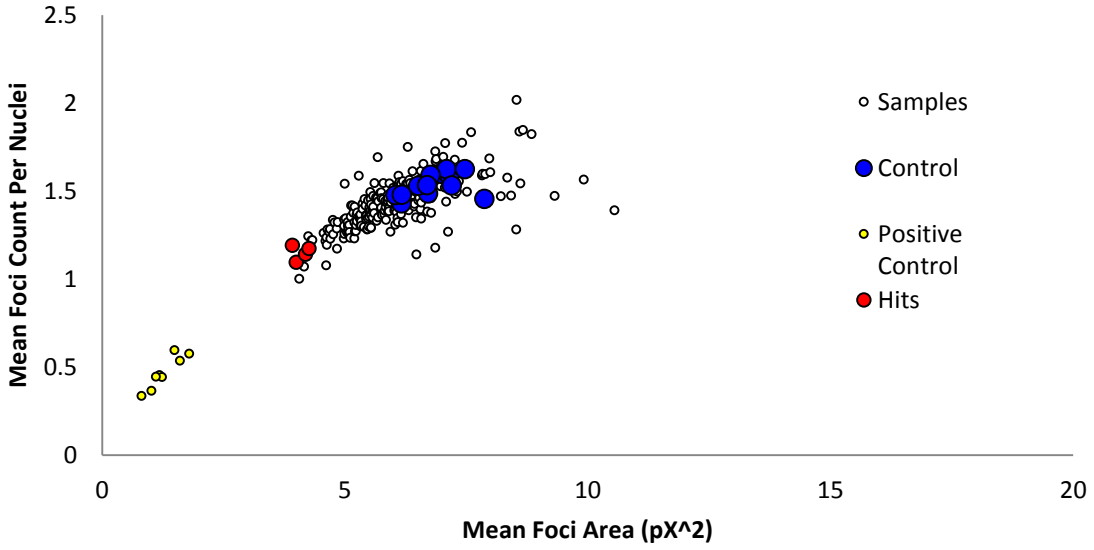

Figure 7: Raw Data from kinome RNAi screen for modulators of foci integrity: Samples scored on number of foci per nuclei (y-axis) versus mean foci area per nuclei (x-axis).

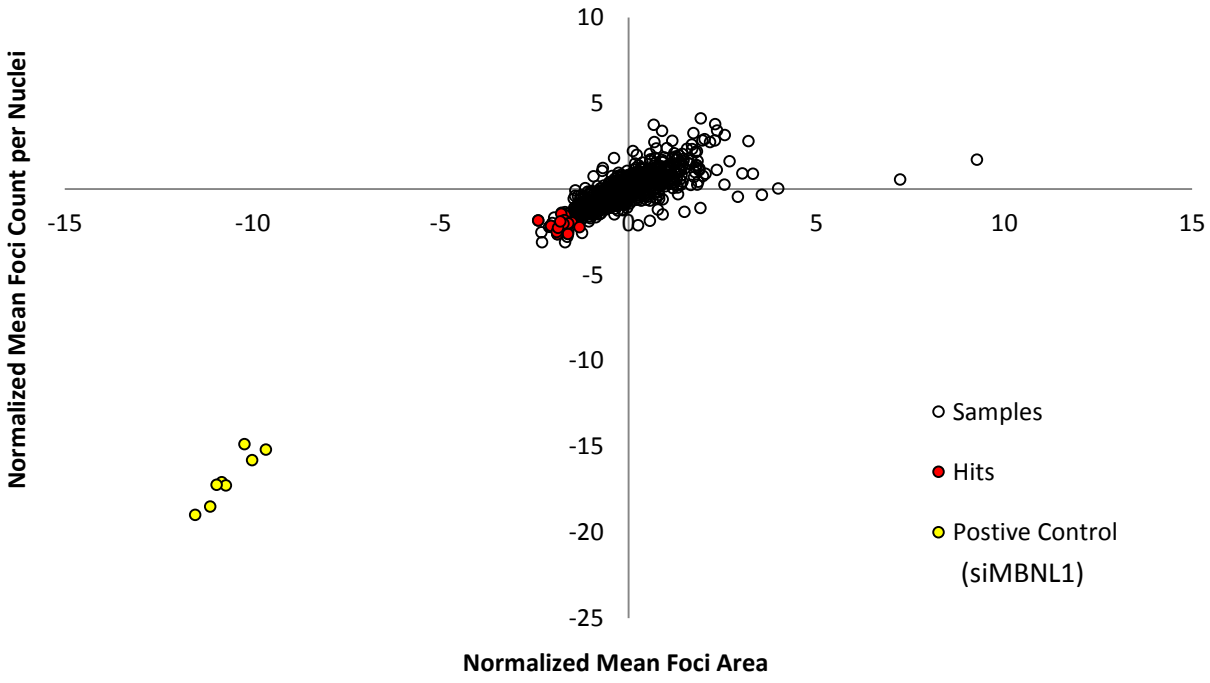

Figure 8: Normalized distribution of kinome screen: Z-scores compiled for each sample for mean foci area and foci count per nuclei. Hits were selected according to proximity to positive control and a mean z-score in either category less than -2.0.

Table 1: Compilation of top kinase hits for DM1 foci screen with associated Z-scores

Gene Name	Foci Surface Area per Nuclei (Mean Z-score)	Foci Count per Nuclei (Mean Z-score)	Description
PRKRA (PACT)	-2.40	-2.17	Interferon-inducible double-stranded RNA dependent activator
IP6K3	-1.81	-2.02	Inositol hexakisphosphate kinase 3
MAST3	-1.87	-2.27	Microtubule associated serine/threonine kinase 3
TLK2	-1.89	-2.65	Tousled-like kinase 2

3.2 PACT

3.2.1 Validation of PACT siRNA sequences

The kinase siRNA library obtained from Qiagen uses a pool of four individual siRNA sequences for each gene, each well thus contains four different siRNAs that target unique areas of a given kinase gene. To confirm the presence of an on-target hit, the four PACT siRNAs were tested individually for their ability to impact nuclear foci. Two of the four siRNAs used in the original screen significantly reduced foci surface area over three independent trials as seen in Figure 9 (*$p<0.05$). The ability of two unique siRNA sequences targeting PACT to affect the nuclear foci size and number indicates that PACT mediate reduction of foci size is likely a real observation and not due to off-target effects.

Further analysis employing PACT siRNA sequences were next conducted. Western blot was performed to assess the level of PACT protein over 96hrs of incubation with PACT siRNA in DM1 500 cells (Figure 10 A). PACT protein levels begin to decrease after 24hrs of incubation with siRNA, and continue to diminish over the course of 96 hrs. The kinetics of foci surface area reduction does not perfectly mirror the decrease in PACT protein, reaching a low point after 48hrs of incubation with siRNA, but begins to rebound over the course of 96hrs (Figure 10 B) while PACT protein levels shows a steady monotonic decrease over this period. Thus the effect of PACT protein levels on nuclear foci is transient; it is clear that the cell adjusts in some fashion to the impact of the decreasing PACT over time.

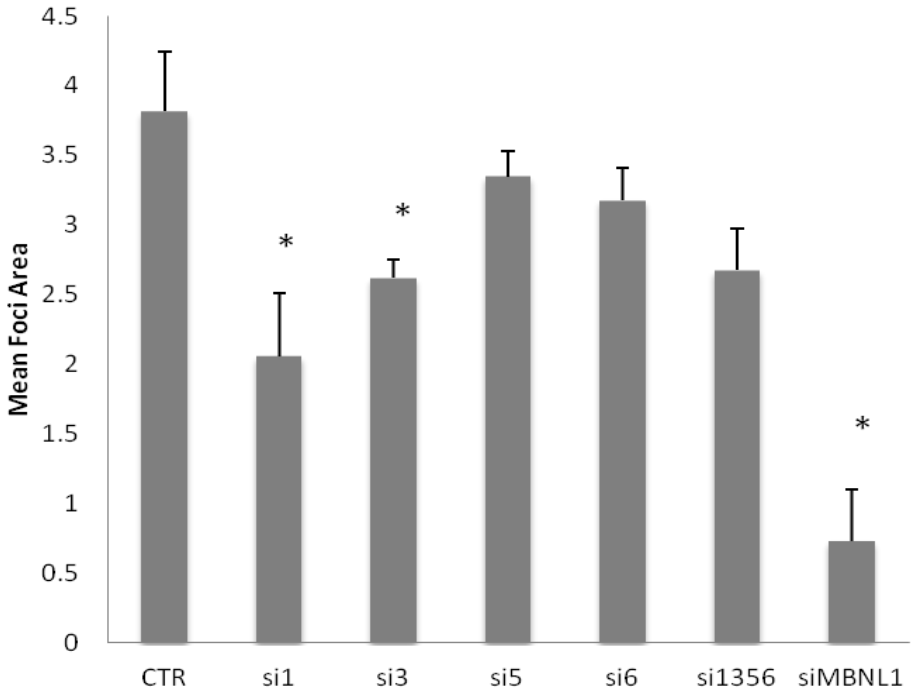

Figure 9: PACT siRNA used in the screen is on target: 2 of 4 siRNAs used for PACT knockdown in the screen significantly reduce foci area in DM1 500 fibroblasts at 48hrs and 20nM. (error bars indicate SEM for n=3) (* $p < 0.05$ compared to CTR).

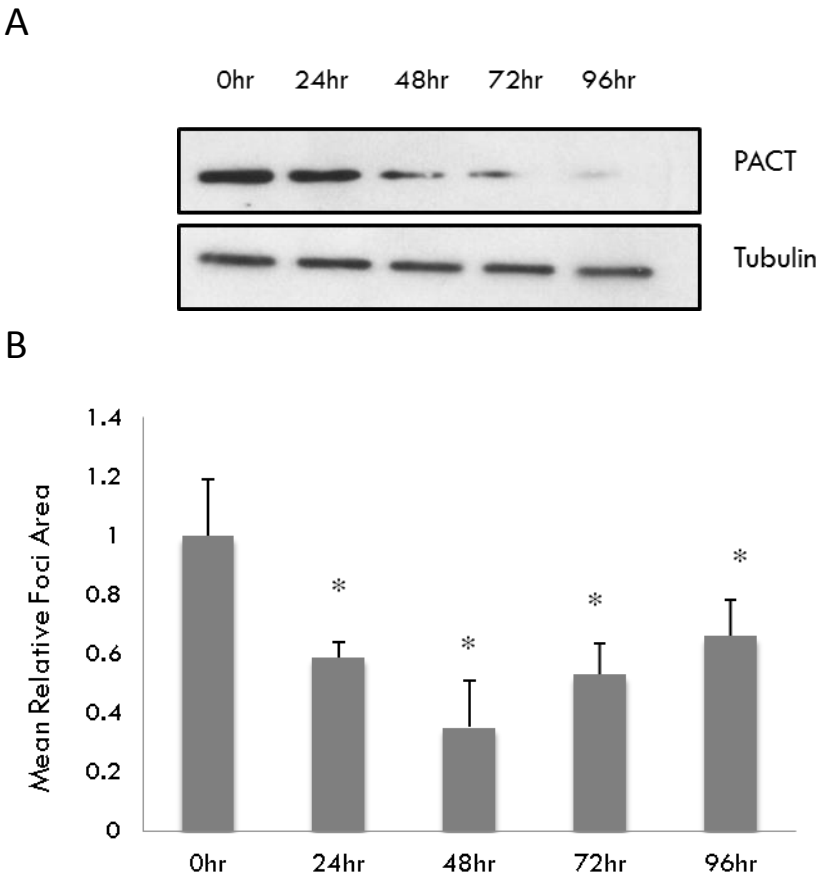

Figure 10: Depletion of PACT protein significantly reduces the formation of nuclear RNA foci: (A) Treatment with PACT siRNA (si 1) over 96hrs of incubation as shown by western Blot (0hr controls are treated with non-targeting control siRNA). (B) Quantification of foci surface area after treatment with PACT siRNA. (error bars indicate SEM for n=3) (* $p < 0.05$).

3.2.2 Assessment of PACT protein knockdown on dsRBPs MBNL1 and CUGBP1

Western blot analysis was performed on DM1 500 cells to investigate the impact of PACT knockdown on other important DM1 biomarkers. PACT knockdown was performed over the course of 96hrs and the levels of MBNL1 and CUGBP1 protein were monitored (Figure 11 A). PACT knockdown causes a robust induction of MBNL1 protein (Figure 11 B). Over the course of three independent treatments of DM1 500 cells with PACT siRNA, MBNL1 protein levels reached nearly 30 times that of controls by 48hrs before beginning to subside. It should be noted that the range of MBNL1 levels over the three trials resulted in a large standard error and thus it is likely, with greater sample size, the true level of MBNL1 protein would be lower. The observed variance results in statistical significance of MBNL1 levels occurring only at 48hrs of incubation with PACT siRNA. We believe that larger sample size may result in greater significance for all time points of MBNL1 levels. This time course mirrors the effect seen in the reduction of nuclear foci with PACT knockdown in Figure 10 B, showing a similar disconnect from PACT protein levels. There is also a modest non-statistically significant ($p<0.07$) reduction in CUGBP1 protein levels at 48hrs of incubation with PACT siRNA, which then increases back to normal levels by 96hrs (Figure 11 C).

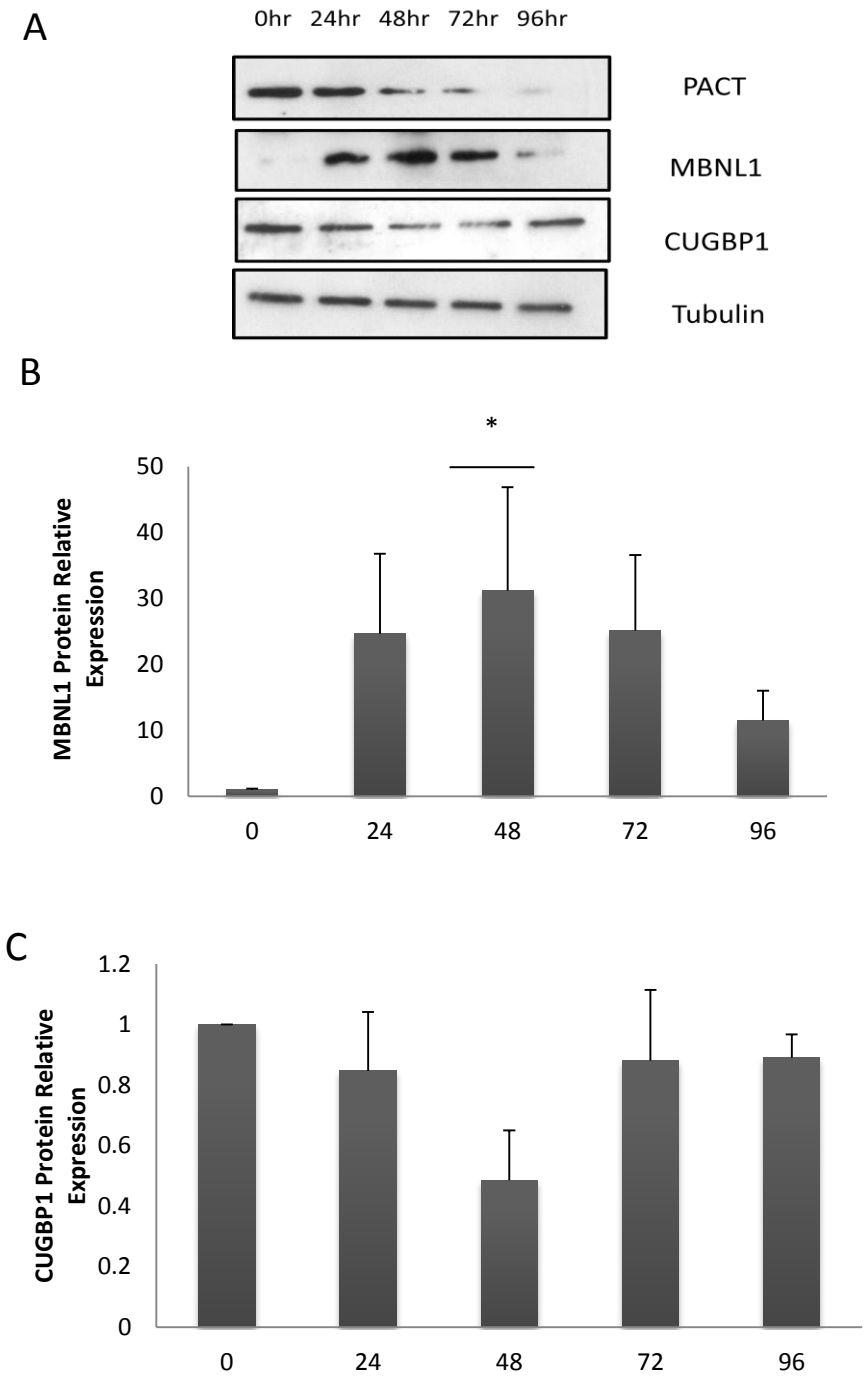

Figure 11: Depletion of PACT protein in DM1 cells increases MBNL1 protein levels while decreasing CUGBP1 protein levels: (A) Representative western Blot of PACT siRNA treatment in DM1 500 fibroblasts over 96hrs (0hr control treated with non-targeting siRNA for 24hrs). (B + C) Quantification of MBNL1/CUGBP1 protein levels in DM1 500 cells by densitometry. (error bars indicate SEM for n=3)(* $p < 0.05$)

3.2.3 Assessment of PACT protein knockdown on DM1-affected mRNA splicing

RT-PCR was used to assess whether the changes observed in MBNL1 and CUGBP1 protein levels result in the normalization of the dysregulated splicing normally observed in DM1. Insulin receptor was used as a readout of splicing regulation due to its prominence in the literature and expression in fibroblasts. Insulin receptor (IR) mRNA was reverse transcribed and then amplified using primers that flank exon 11, resulting in the formation of two PCR products. Transcription of the smaller isoform, containing no exon 11 has been well documented in DM1 and is thought to underlie the insulin resistance observed in the condition (Dansithong et al., 2005). Treatment of DM1 2000 cells with PACT siRNA resulted in increased inclusion of exon 11 with the maximum effect seen at 48hrs (Figure 12 A), consistent with the increased levels of MBNL1.

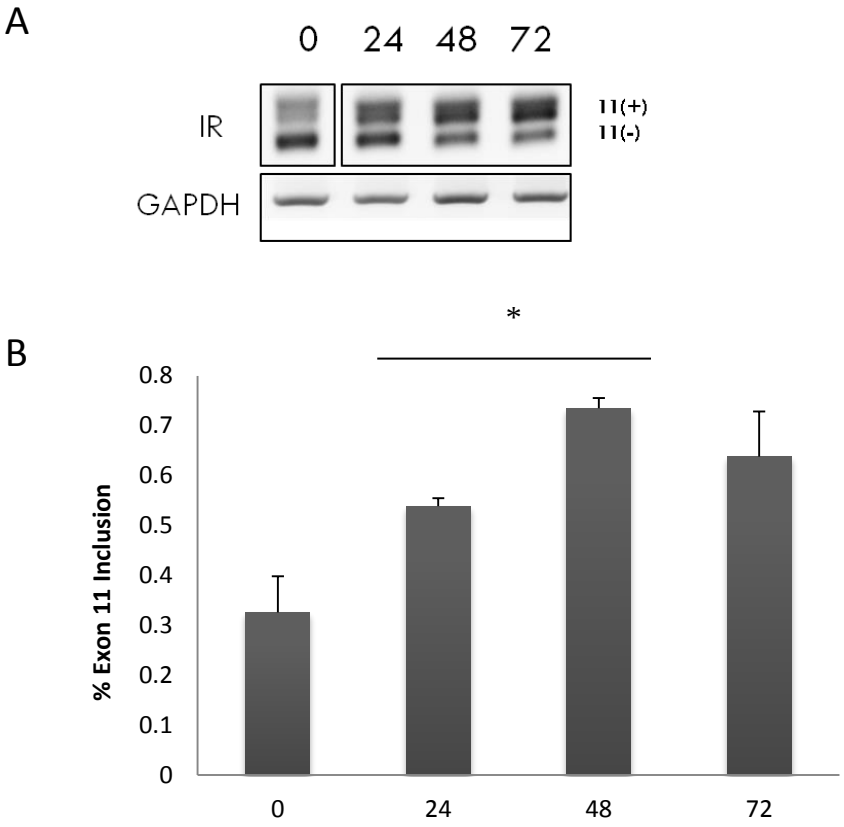

Figure 12: Treatment with PACT siRNA increases the inclusion of exon 11 in the insulin receptor mRNA: (A) Representative agarose gel electrophoresis of RT-PCR amplification of insulin receptor mRNA with GAPDH loading control, RNA isolated after DM1 2000 fibroblasts and normal human fibroblasts incubated with PACT siRNA (0hr control treated with non-targeting siRNA for 24hrs). (B) Quantification of the ratio of exon 11 inclusion in the insulin receptor transcript. (error bars indicate SEM for n=3)(* $p<0.05$)

3.2.4 PACT knockdown in normal human fibroblasts

Treatment of normal human fibroblasts (NHF) with PACT siRNA was performed to determine whether the effect on splicing proteins MBNL1 and CUGBP1 was contingent upon knockdown of DM1 nuclear foci. A western blot was performed comparing levels of MBNL1 protein in NHF cells following 48 hours of treatment with PACT siRNA (Figure 13 A). A significant and robust induction of MBNL1, albeit somewhat less than that observed in DM1 cells, was observed over the course of three experiments, resulting in levels over eight times higher than controls (Figure 13 B). This demonstrates that the effect of PACT knockdown on MBNL1 expression is not specific to DM1 cells, and is, to some degree, independent of DM1 nuclear foci reduction.

The impact of PACT knockdown on IR receptor isoforms was also examined in NHF cells. RT-PCR was performed after NHF and DM1 500 cells were incubated with PACT siRNA (Figure 14 A). A significant difference in the percentage of exon 11 inclusion was found between NHF and DM1 cells treated with control siRNA. An increase in the inclusion of exon 11 was observed in NHF cells following treatment with PACT siRNA, though not to the same extent as in DM1 cells. This further demonstrates that the effect of PACT in DM1 cells is independent of its modulation of nuclear foci.

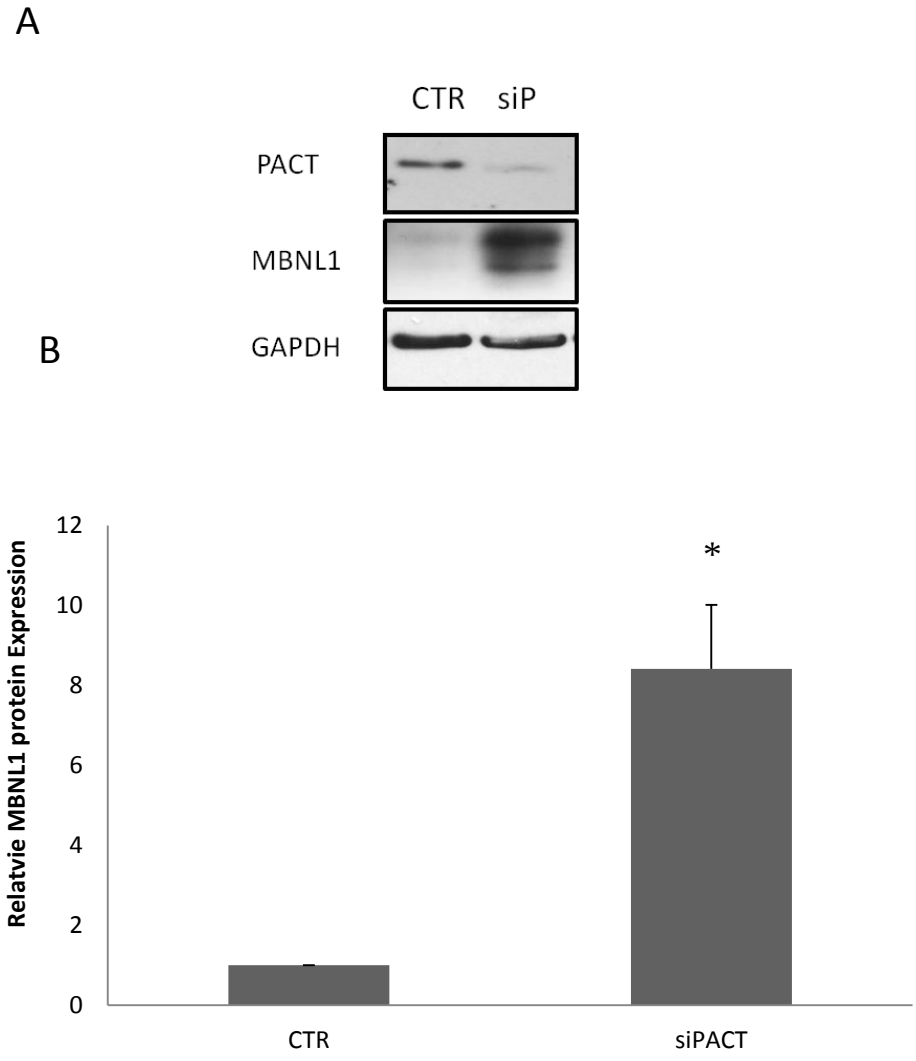

Figure 13: MBNL1 induction resulting PACT knockdown is not wholly DM1 specific: (A) Representative western blot of MBNL1 induction in NHF cells with GAPDH loading control, cells were transfected with either PACT siRNA or non-targeting siRNA (CTR) and harvested after 72hrs. (B) Quantification of MBNL1 induction in NHF cells treated with PACT siRNA (error bars indicate SEM for n=3) (* $p < 0.01$)

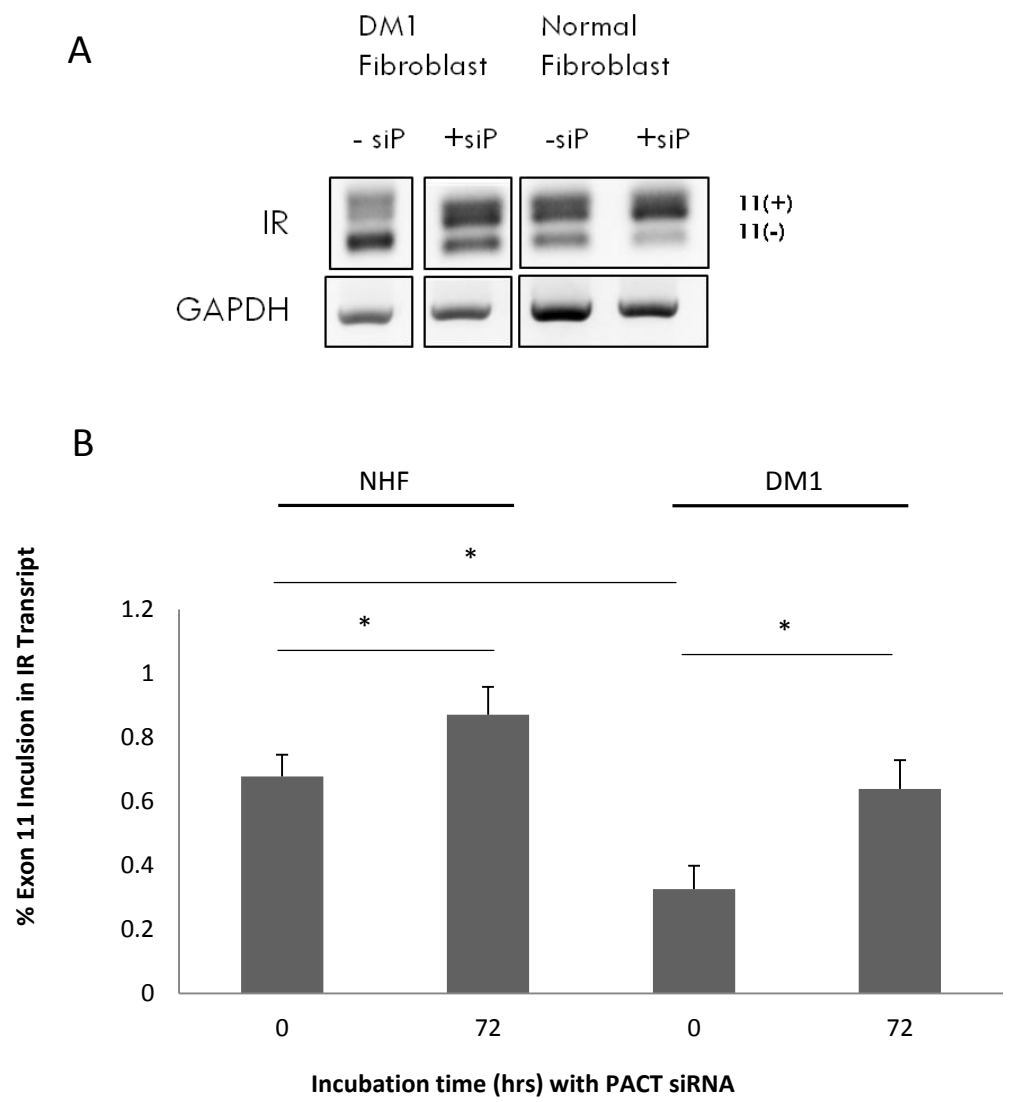

Figure 14: The impact of PACT RNAi on insulin receptor splicing are not wholly DM1 specific: (A) Representative agarose gel electrophoresis of RT-PCR amplification of IR mRNA and GAPDH, mRNA isolated after DM1 2000 fibroblasts and normal human fibroblasts were incubated with PACT siRNA (0hr control treated with non-targeting siRNA for 24hrs). (B) Quantification of the ratio of exon 11 inclusion in the insulin receptor transcript. (error bars indicate SEM for n=2)(* $p<0.05$)

3.3 TRBP

As outlined in chapter 1, TRBP is a highly homologous binding partner of PACT. To gain further insight into the mode of action of PACT, knockdown of TRBP was performed. DM1 500 cells were incubated with TRBP siRNA for 72hrs and RT-PCR was used to confirm knockdown (Figure 15 A). Robust induction of MBNL1 was observed following knockdown of TRBP, as evidenced by western blot in Figure 15 B. Reduced expression of Dicer a protein known to bind both TRBP and PACT, was also observed following TRBP knockdown. Furthermore, knockdown of TRBP produced a reduction in the surface area of nuclear foci at 72hrs that was similar to the effect of PACT knockdown (Figure 15 C). The combination of PACT and TRBP siRNA produced a similar knockdown of foci, neither greater nor less than that observed with PACT or TRBP knockdown individually, suggesting that the impact of the two knockdowns may be by the same pathway.

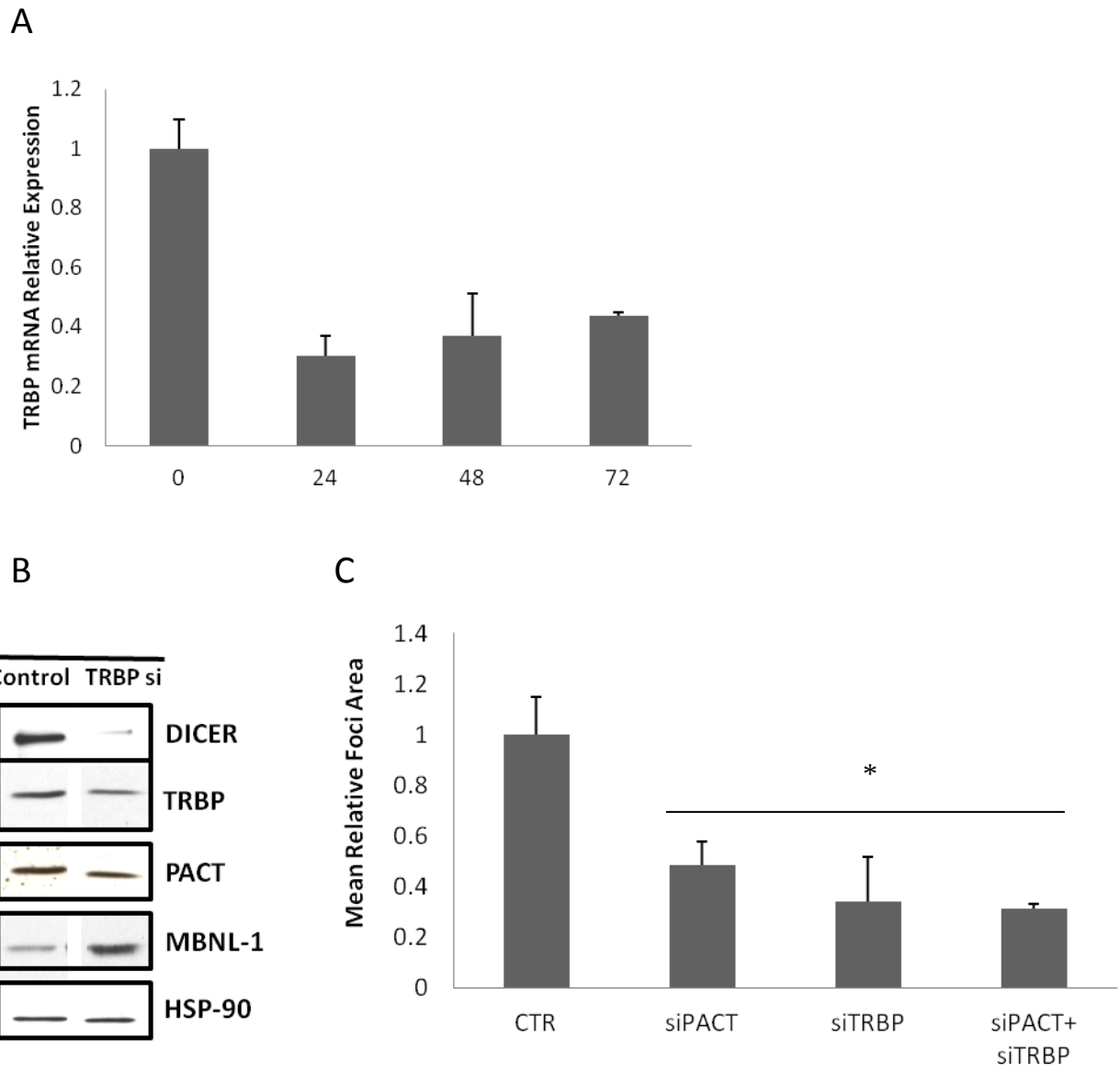

Figure 15: TRBP knockdown induces MBNL1 expression and foci knockdown in DM1 cells: (A) TRBP siRNA knocks down TRBP mRNA expression over 72hrs: qPCR quantification of TRBP mRNA knockdown using siRNA, DM1 500 cells were treated with TRBP siRNA (20nM) and total RNA was extracted. (0hr controls were treated with non-targeting siRNA) (B) TRBP knockdown induces MBNL1 expression: western blot demonstrating protein levels for DICER, TRBP, PACT, MBNL1, and HSP-90 upon treatment of DM1 500 cells with TRBP siRNA for 48hrs. (C) Both PACT and TRBP knockdown reduce foci surface area, and their combination has no additive effects: quantification of foci surface area of DM1 500 cells treated with CTR siRNA, PACT siRNA, TRBP siRNA, and the combination of PACT and TRBP siRNA.

3.4 RNAi enhancing compounds

The similar impact of PACT and TRBP RNAi on DM1 biomarkers raised the possibility of a shared mechanism of action, possibly involving their common interaction with DICER. To this end, two Dicer activating fluoroquinolone compounds enoxacin and ciprofloxacin were identified and tested for their ability to induce MBNL1 protein (Shan et al., 2008; Melo et al., 2011). Western blots were performed on MBNL1 protein after DM1 cells were treated with 0.1, 0.5 and 1.0 μM of each compound (Figure 16 A-B). A mild induction of MBNL1 protein was observed for both compounds after 72hrs of treatment (Figure 16 C-D). However, no effect was found on the surface area of foci for any concentration of either compound (Figure 16 E-F). This may indicate that the induction of MBNL1 and the reduction of nuclear foci are independent events in the knockdown of both PACT and TRBP.

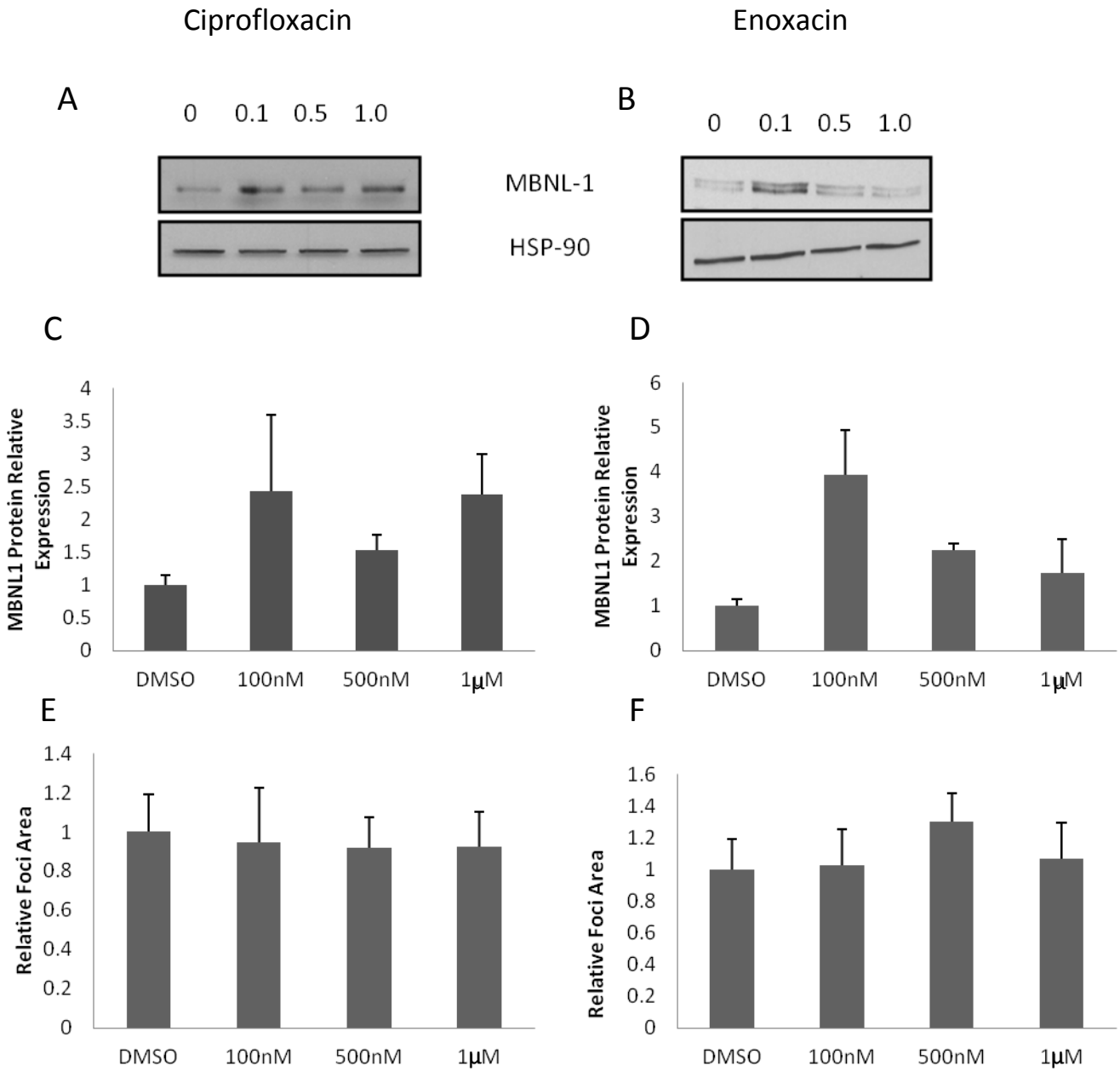

Figure 16: RNA Interference enhancing compounds may induce MBNL1 expression but have no effect on nuclear foci area: (A-B) Western blot of drug treatments: DM1 500 cells were treated with 0, 0.1, 0.5, and 1.0 μM ciprofloxacin and enoxacin respectively, for 72hrs. 0 μM control was treated with 0.5% DMSO. (C-D) Quantification of MBNL1 levels compared to HSP-90 loading control. (E-F) Quantification of foci area relative to controls following 72hr drug treatment. (error bars indicate SEM for n=2)

3.4 PKR inhibitor

PACT and TRBP both interact with, but have opposing effects on, PKR. PACT is an activator of PKR while TRBP is an inhibitor. Given the similar effect of PACT and TRBP knockdown, it is thus unlikely that they are acting through PKR. To discount this possibility, we used a selective PKR inhibiting compound imidazole oxindole C16. DM1 cells were treated with varying concentrations of the compound for 24hrs, while controls were treated with DMSO. We observed a reduction in the size of nuclear foci after treatment with the PKR inhibitor (Figure 17 A). To confirm that PKR phosphorylation was reduced, we assessed levels of phospho-PKR by western blot (Figure 17 B). Interestingly, no induction of MBNL1 was observed after treatment with the PKR inhibitor.

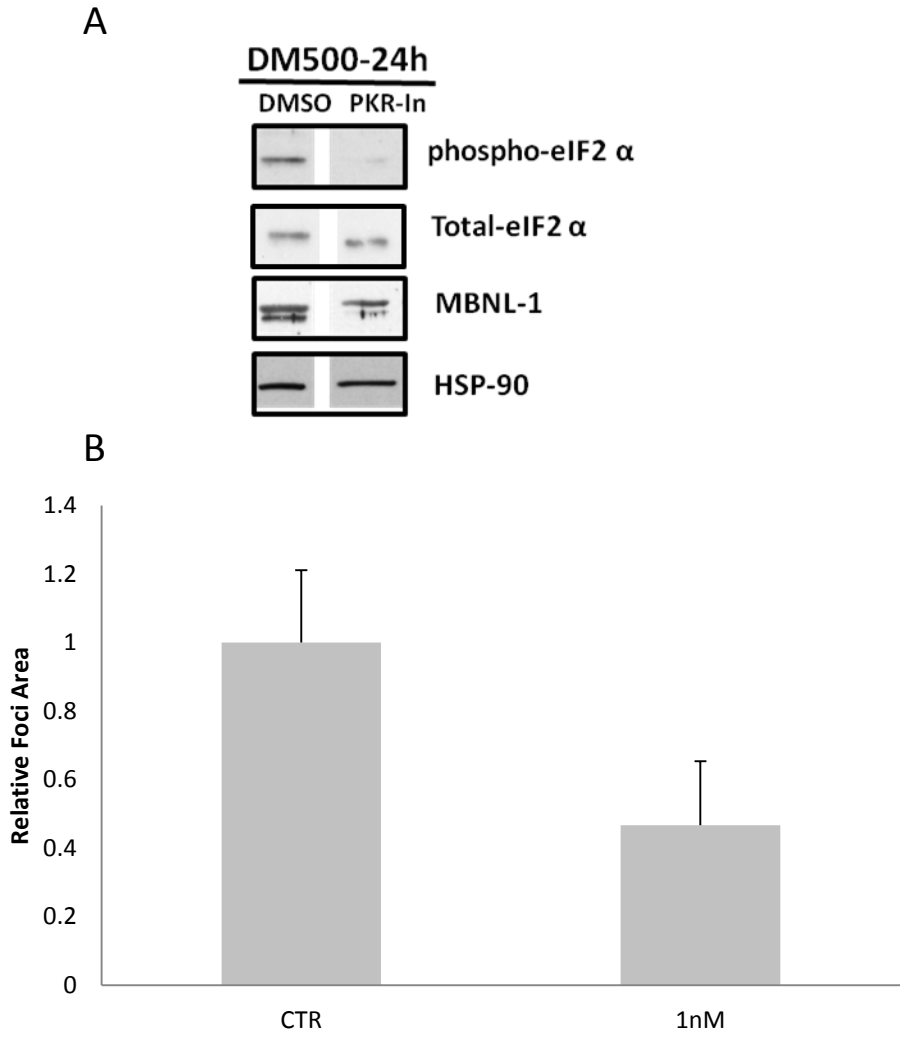

Figure 17: PKR inhibition causes reduction in foci size but does not induce MBNL1: (A) Western blot demonstrating decreased phosphorylation of eIF2a following treatment of DM1 500 cells with 1nM of PKR inhibitor oxindole imidazole derivative C16. (B) Quantification of foci surface are following treatment of DM1 500 cells with PKR inhibitor C16 for 24 hours at varying concentrations. (error bars represent SEM for n=2).

Chapter 4

4. Discussion

4.1 Major Findings

Myotonic Dystrophy type 1 is a common muscular dystrophy for which there is no effective treatment. The generation of new treatment strategies and discovery of potential therapeutic targets for genetic disorders is the focus of our laboratory. The purpose of our study is to identify protein kinases that have the ability, when inhibited, to reduce the size and number of toxic nuclear foci that are believed to be the chief source of pathogenesis in DM1 cells. Our hope is to identify new targets for therapeutics as well as attempt to find compounds known to modify any kinases we may identify, and test their potential for DM1 treatment. This approach has the potential to uncover significant new information on the dynamics of DM1 nuclear foci and the factors that may affect their formation or dissolution.

4.2 High-throughput Screening

4.2.1 Screen Development

The generation of a high-throughput RNAi screen for DM1 cells required thorough optimization of *in situ* hybridization as well as cell culture and transfection conditions. A cell line with a strong signal from nuclear foci was necessary for the effective quantification of their size and number. Patient skin fibroblasts expressing 500 CTG repeats were selected for meeting several of these criteria and for their ease of care in culture. The DM1 500 cells express nuclear foci to a moderate degree, as seen in Figure 2 middle panel, but are easily distinguishable from

non-DM1 cells. The quantification of nuclear foci in Figure 3 demonstrates the different degree of foci expression between cell lines. The increased surface area of nuclear foci in DM1 2000 cell line compared to the DM1 500 line confirms that nuclear foci are a suitable readout of disease severity and allows us to use our screen to identify moderation in severity by reduction in foci. Characterization of the cell line for screening involved the determination of transfection efficiency and control selection. The transfection efficiency of DM1 500 cells was determined, using a cell death inducing control siRNA called ALLSTAR Death. Cells treated with the ALLSTAR siRNA had a survival rate of 20% after 96 hours incubation, indicating approximately 80% transfection efficiency in DM1 cells (Figure 4).

Selection of appropriate controls is another important step in setting up a robust genetic screen. A strong positive control is helpful in the selection of hits and for confirmantion that the assay is working properly. We chose MBNL1 siRNA as our positive control due to its necessity in the formation of nuclear foci (Dansithong et al., 2005). MBNL1 is segregated from the nucleoplasm by binding to mutant DMPK mRNA and is a principle component of nuclear foci. The use of MBNL1 siRNA effectively reduces the number and size of nuclear foci in DM1 cells as the levels of MBNL1 protein are reduced, providing a very strong control (Figures 5 and 6).

It is important to note that the selection of cell line introduces bias into the screening process as transcript expression levels are not well established for the siRNA library target genes (Birmingham et al., 2009). Therefore, the assay may be skewed toward the identification of genes that may have less importance in other cell types. Other parameters of the screen also introduce bias. Particularly, the use of bioinformatic sequence generation for the design of siRNA molecules in a large library has the potential for off-target effects. The largely unvalidated set of siRNAs used in the screen has the ability to introduce false positives in the

case of off-target effects, where the generated sequence affects the expression of more transcripts than the intended target alone (Perrimon and Mathey-Prevot, 2007). Furthermore, the variability of transcript stability and protein degradation accross the library does not guarantee that at the timepoint of assaying (96 hours), all targeted proteins have been knocked down. Many proteins may have returned to their original levels, or may display a delayed knockdown outside the window of assaying, both of which may produce false negatives.

4.2.2 Data Analysis

In total, 512 protein kinases were screened in triplicate from the siRNA library obtained from Qiagen. Each plate was assessed for the presence of edging and drift effects that may introduce bias. In culture, it is possible for the growth conditions across a large plate to be heterogenous, which may impact the screening phenotype. Initial screening of individual plates demonstrated mild drift effects, causing one side of the plate to demonstrate higher foci values than the other. This could be due to growth conditions, or the non-uniform dispensing of assay reagents. The raw data was compiled for each plate based on the mean number of foci found per nuclei and the mean foci surface area per nuclei (example Figure 7). It was apparent upon viewing the distribution of data for each plate, that the non-targeting control siRNA group did not fall in the middle of the sample distribution, but was skewed toward higher values. The data were then normalized by calculating the Z-score value for each sample. This returns a value indicating the number of standard deviations from the sample mean that a given sample falls. Note that this is calculated using the mean of all samples, rather than the mean of non-targeting control siRNA treated cells in order to get a more accurate measure of the middle of the

distribution. Using the non-targeting control siRNA as our mean would result in a greater number of hits, due to their higher values.

Cross-plate Z-scores were compiled for all samples for foci values as well as nuclei count. Nuclei count was then used to eliminate any lethal kinases from the data set. Mean Z-scores of -3.0 for nuclei count or lower accross three replicates were considered to be lethal and rejected from further analysis. The remaining data set was then ranked according to Z-score and samples with a mean Z-score less than -2.0 in either foci area or foci number were selected as hits (Figure 8). The cutoff of -2.0 was used as 96% of the data should lie within two standard deviations of the mean (Birmingham et al., 2009). As with other normalization techniques, there remains a possibility of false positives and false negatives.

We concentrated on lower Z-score values rather than values greater than 2.0 due to the our focus on therapeutic targets. We have made the assumption in our strategy that the knockdown of a protein is akin to inhibition of its function, and that kinases that we identify in our screen that reduce the number of foci when knocked down may represent therapeutic targets for selective kinase inhibitors. While this may not ultimately be the case, we believe the therapeutic potential is greater than studying kinases that when inhibited, increase the number of foci. Furthermore, we found that our assay detected fewer outliers in this area. There were fewer samples that decreased the size and number of foci than increased, as seen in Figure 8. Though there may be the potential for the discovery of new biological interactions in DM1 with foci increasing proteins, we are more focussed on the search for therapeutic targets.

The parameters for screening resulted in the identification of four kinase hits with the ability to reduce foci number and size (Table 1). A screening of the literature led to the focus on

PACT in particular given its' association with PKR, that has been previously studied in relation to DM1 (Mankodi et al., 2003).

4.3 PACT as a Modulator of DM1 Biomarkers

4.3.1 PKR

The identification of PACT in our screen and its association with double-stranded RNA activated protein kinase (PKR) made it an attractive candidate for further study. PKR was first associated with DM1 as a candidate for interaction with CUG expanded mRNAs. Tian and colleagues (2000) found that expression of expanded CUG repeat mRNAs formed hairpin secondary structures that had the ability to activate PKR. Furthermore, they demonstrated that CUG repeats greater than 15 triplets in length bind to PKR through its dsRNA-binding domain *in vitro,* thereby activating PKR. This gain of function of DMPK RNA was proposed to act through PKR in the development of cellular stress. The exact role that PKR plays in DM1 is still not well understood. PKR knockout mice were generated and crossed with a DM1 mouse model, that displayed no changes in disease development, calling into question the significance of the interaction between DMPK mRNA and PKR in DM1 (Mankodi et al., 2003). Other groups have demonstrated that that expression of expanded CUG mRNA can inhibit protein synthesis in cis and in trans, though these knockout experiments demonstrated that the effect cannot be completely attributed to PKR (Tian et al., 2005). Studies have since shown significant changes in cell transcriptomes based on the introduction of expanded CUG mRNA as well as the activation of genes that interact with ds-RNA and interferon-regulated genes, particularly in DM1 patients cataracts (Rhodes et al., 2012). The focus of these DM1 investigations on PKR made the PKR-

activating protein, PACT, an intriguing hit in our screen and supports these previous findings of a role for PKR in the pathogenesis and activation of apoptosis in DM1.

4.3.2 PACT

PACT is known to interact with PKR as an activator during cellular stresses and can mediate diverse gene induction and apoptosis (Marques et al., 2008). PACT binds with TRBP during normal conditions, but cellular stress causes the dissociation of the PACT-TRBP complex, allowing PACT to activate PKR by phosphorylation (Singh and Patel, 2012). PACT and TRBP are also both active in RNAi pathways through association with Dicer, and recently there has been evidence that they facilitate strand selection for siRNA and miRNA targets (Lee et al., 2013; Takahashi et al., 2013).

Upon secondary validation from our screen, we found that PACT significantly modulates the expression of DM1 nuclear foci. Treatment with PACT siRNA consistently knocks down the expression of foci in DM1 500 cells and induces the induction of MBNL1 protein (Figures 10 and 11) which confers changes in the expression of insulin receptor isoforms (Figure 12). The levels of MBNL1 induction reported are likely inflated due to the high error reported. However, we are confident that robust MBNL1 induction is occurring consistently with PACT modulation. These changes observed in DM1 cells signify the clinical potential of PACT as a target, as MBNL1 overexpression has been demonstrated to reverse RNA missplicing and myotonia in a DM1 mouse (Kanadia et al., 2006). We have also shown that this induction of MBNL1 and splicing changes are not unique to cells expressing nuclear foci (Figures 13 and 14), confirming

that the mechanism underlying the induction of MBNL1 is not dependent on the presence of expanded CUG hairpins.

We hypothesized initially that the effect on foci and MBNL1 from PACT knockdown could potentially be mediated by TRBP, as knockdown of PACT could possibly increase levels of free TRBP. We performed siRNA knockdown of TRBP and, unexpectedly, found similar effects as PACT knockdown, where TRBP depleted cells had lower foci surface area and increased MBNL1 levels (Figure 15). Interestingly, the combination of TRBP and PACT siRNAs produced no amplification of the effect nor abrogation. This is in disagreement with several findings on the antagonistic role of TRBP and PACT in the activation of PKR and Dicer processing (Singh and Patel, 2012; Takahashi et al., 2013). It is possible that in this particular process, PACT and TRBP knockdown produces a similar effect in the cell that is independent of their roles in PKR activation and Dicer processing. Due to the activation of PKR in DM1 cells, we believed that the effects mediated by PACT siRNA may have been attributable to reduced activation of PKR. However, our results with TRBP knockdown in DM1 cells points to a different cause given the antagonistic effects of TRBP and PACT on PKR. To confirm the absence of PKR involvement in the amelioration of DM1 biomarkers during PACT knockdown, we tested the effects of selective inhibition of PKR. Following treatment with an imidazole oxindole C16 PKR inhibitor, we found that foci levels were reduced in DM1 500 cells. This may indicate that PKR is directly or indirectly involved in the sequestration of expanded CUG hairpins. However, from western blot, it is clear that PKR inhibition does not confer induction of MBNL1 protein.

The association of both PACT and TRBP with Dicer led us to consider the modification of miRNA and siRNA processing during RNA interference as a source of the induction of

MBNL1. It has recently been shown that PACT and TRBP have distinct effects on substrate processing by Dicer. PACT in complex with Dicer was found to inhibit processing of siRNAs compared to Dicer-TRBP complexes (Lee et al., 2013) and another group found that TRBP has a higher affinity for siRNA than PACT (Takahashi et al., 2013). Furthermore, miRNA alterations have been documented in both drosophila and human DM1 models where expression of CUG hairpins caused alteration in the expression of miR 1, 7, and 10, and where MBNL1is necessary for the regulation of miR-1 and 7 in Drosophila (Fernandez-Costa et al., 2012), while misregulation of miR-1 has independently been associated with heart defects (Rau et al., 2011). They also reported increased lifespan in Drosophila following over-expression of miR-10 (Fernandez-Costa et al., 2012). With this in mind, we hypothesized that the disruption or enhancement of Dicer target processing may be at the source of MBNL1 induction in our work. Emphasizing the search for therapeutics we searched the literature for Dicer targeting compounds. In doing so we found a class of fluoroquinolone antibiotics that have been shown to increase RNAi processing (Shan et al., 2008; Melo et al., 2011). We tested the effects of both enoxacin and ciprofloxacin on the induction of MBNL1 in DM1 500 cells and found them to produce modest increases in the expression of the protein. There is, however, a large discrepancy between the levels of MBNL1 induction observed during the knockdown of PACT and those observed during treatment with ciprofloxacin and enoxacin pointing to additional mechanisms in the former case. This may be attributable to modest activation of RNAi pathways that may be enhanced during targeting of PACT or TRBP with siRNA. Furthermore, we are unsure of the validity of this approach using RNAi enhancing compounds, as we have demonstrated that Dicer levels are markedly reduced during the knockdown of TRBP.

4.4 Conclusions

The antagonistic roles of TRBP and PACT on PKR activation as well as during strand selection for Dicer substrates indicates a disconnect in our results. We have found that modulation of foci levels can be achieved by inhibition of PKR, through PACT knockdown, or TRBP knockdown. We believe this effect to be principally due to increased inhibition of PKR, though inhibition of PKR alone is not sufficient to enhance MBNL1 levels. Similarly, we have found that both PACT and TRBP knockdown can induce levels of MBNL1 protein. We believe the evidence of MBNL1 induction with RNAi enhancing compounds suggests that this effect may be mediated, at least in part, by Dicer. The disruption of PACT and TRBP association with Dicer by siRNA knockdown may affect MBNL1 levels, possibly through modulation of several miRNAs. The potential therapeutic value of enoxacin and ciprofloxacin may still be in question, but we believe that we have demonstrated that targeting of RNAi pathways or PKR represent novel targets for DM1 therapy. Furthermore, we believe that this example of mechanistically informed reversion of a monogenic disease cellular phenotype can be used as a model for novel therapeutic interventions for rare genetic disease.

Chapter 5

5. References

Amack, J.D., S.R. Reagan, and M.S. Mahadevan. 2002. Mutant DMPK 3'-UTR transcripts disrupt C2C12 myogenic differentiation by compromising MyoD. *J.Cell Biol.* 159:419-429.

Benders, A.A., P.J. Groenen, F.T. Oerlemans, J.H. Veerkamp, and B. Wieringa. 1997. Myotonic dystrophy protein kinase is involved in the modulation of the Ca2+ homeostasis in skeletal muscle cells. *J.Clin.Invest.* 100:1440-1447.

Berul, C.I., C.T. Maguire, M.J. Aronovitz, J. Greenwood, C. Miller, J. Gehrmann, D. Housman, M.E. Mendelsohn, and S. Reddy. 1999. DMPK dosage alterations result in atrioventricular conduction abnormalities in a mouse myotonic dystrophy model. *J.Clin.Invest.* 103:R1-7.

Birmingham, A., Selfors, L. M., Forster, T., Wrobel, D., Kennedy, C. J., Shanks, E., Shamu, C. E. (2009). Statistical methods for analysis of high- throughput RNA interference screens. *Nature Methods. 6*(8), 569–575.

Boutros, M., & Ahringer, J. (2008). The art and design of genetic screens: RNA interference. *Nature reviews. Genetics*. *9*(7), 554–66.

Brook, J.D., M.E. McCurrach, H.G. Harley, A.J. Buckler, D. Church, H. Aburatani, K. Hunter, V.P. Stanton, J.P. Thirion, and T. Hudson. 1992. Molecular basis of myotonic dystrophy: expansion of a trinucleotide (CTG) repeat at the 3' end of a transcript encoding a protein kinase family member. *Cell*. 68:799-808.

Brouwer, J.R., R. Willemsen, and B.A. Oostra. 2009. Microsatellite repeat instability and neurological disease. *BioEssays : News and Reviews in Molecular, Cellular and Developmental Biology*. 31:71-83.

Carrasco, M., J. Canicio, M. Palacin, A. Zorzano, and P. Kaliman. 2002. Identification of intracellular signaling pathways that induce myotonic dystrophy protein kinase expression during myogenesis. *Endocrinology.* 143:3017-3025.

Chamberlain, C.M. and L.P. Ranum (2012). Mouse model of Muscleblindlike-1 overexpression: skeletal muscle effects and therapeutic promise. *Hum mol gen.* 21(21): 4645-4654.

Cooper, T. and Lee (2009). Chemical reversal of the RNA gain of function in myotonic dystrophy. *PNAS. 106*(44), 18433–4.

Daniels, S. M., & Gatignol, A. (2012). The multiple functions of TRBP, at the hub of cell responses to viruses, stress, and cancer. *MMBR. 76*(3), 652–66.

Dansithong, W., Wolf, C. M., Sarkar, P., Paul, S., Chiang, A., Holt, I., … Reddy, S. (2008). Cytoplasmic CUG RNA foci are insufficient to elicit key DM1 features. *PloS one*. *3*(12), e3968.

Dansithong, Warunee, Sharan Paul, Lucio Comai, and S. R. (2005). MBNL1 is the Primary Determinant of Focus Formation and Aberrant Insulin Receptor Splicing in DM1. *J. Biological chemistry*, *280*(7), 5773–5780.

Davis, B.M., M.E. McCurrach, K.L. Taneja, R.H. Singer, and D.E. Housman. 1997. Expansion of a CUG trinucleotide repeat in the 3' untranslated region of myotonic dystrophy protein kinase transcripts results in nuclear retention of transcripts. *PNAS*. 94:7388-7393.

De Haro, M., Al-Ramahi, I., De Gouyon, B., Ukani, L., Rosa, A., Faustino, N. A., … Botas, J. (2006). MBNL1 and CUGBP1 modify expanded CUG-induced toxicity in a Drosophila model of myotonic dystrophy type 1. *Human molecular genetics*. *15*(13), 2138–45.

Du, H., Cline, M. S., Osborne, R. J., Tuttle, D. L., Clark, T. a, Donohue, J. P., … Ares, M. (2010). Aberrant alternative splicing and extracellular matrix gene expression in mouse models of myotonic dystrophy. *Nature structural & molecular biology*. *17*(2), 187–93.

Ebralidze, A., Y. Wang, V. Petkova, K. Ebralidse, and R.P. Junghans. 2004. RNA leaching of transcription factors disrupts transcription in myotonic dystrophy. *Science.* 303:383-387.

Fardaei, M., Rogers, M. T., Thorpe, H. M., Larkin, K., Hamshere, M. G., Harper, P. S., & Brook, J. D. (2002). Three proteins, MBNL, MBLL and MBXL, co-localize in vivo with nuclear foci of expanded-repeat transcripts in DM1 and DM2 cells. *Human molecular genetics* *11*(7), 805–814.

Fernandez-Costa, J. M., Garcia-Lopez, A., Zuñiga, S., Fernandez-Pedrosa, V., Felipo-Benavent, A., Mata, M., … Artero, R. D. (2013). Expanded CTG repeats trigger miRNA alterations in Drosophila that are conserved in myotonic dystrophy type 1 patients. *Human molecular genetics*, *22*(4), 704–16.

Furling, D., G. Doucet, M.A. Langlois, L. Timchenko, E. Belanger, L. Cossette, and J. Puymirat. 2003. Viral vector producing antisense RNA restores myotonic dystrophy myoblast functions. *Gene Ther*. 10:795-802.

Furling, D., Lemieux, D., Taneja, K., & Puymirat, J. (2001). Decreased levels of myotonic dystrophy protein kinase (DMPK) and delayed differentiation in human myotonic dystrophy myoblasts. *Neuromuscular disorders : NMD*, *11*(8), 728–35.

Fu, Y.H., D.L. Friedman, S. Richards, J.A. Pearlman, R.A. Gibbs, A. Pizzuti, T. Ashizawa, M.B. Perryman, G. Scarlato, and R.G. Fenwick Jr. 1993. Decreased expression of myotonin-protein kinase messenger RNA and protein in adult form of myotonic dystrophy. *Science.* 260:235-238.

Galka-Marciniak, P., Urbanek, M. O., & Krzyzosiak, W. J. (2012). Triplet repeats in transcripts: structural insights into RNA toxicity. *Biological chemistry*, *393*(11), 1299–315.

García-López, A., Llamusí, B., Orzáez, M., Pérez-Payá, E., & Artero, R. D. (2011). In vivo discovery of a peptide that prevents CUG-RNA hairpin formation and reverses RNA toxicity in myotonic dystrophy models. *PNAS. 108*(29), 11866–71.

Giagnacovo, M., Malatesta, M., Cardani, R., Meola, G., & Pellicciari, C. (2012). Nuclear ribonucleoprotein-containing foci increase in size in non-dividing cells from patients with myotonic dystrophy type 2. *Histochemistry and cell biology*. *138*(4), 699–707.

Harley, H.G., S.A. Rundle, W. Reardon, J. Myring, S. Crow, J.D. Brook, P.S. Harper, and D.J. Shaw. 1992. Unstable DNA sequence in myotonic dystrophy. *Lancet.* 339:1125-1128.

Harmon, E.B., M.L. Harmon, T.D. Larsen, A.F. Paulson, and M.B. Perryman. 2008. Myotonic dystrophy protein kinase is expressed in embryonic myocytes and is required for myotube formation. *Dev.Dyn*. 237:2353-2366.

Harper, P. 2001. Myotonic Dystrophy. W.B Saunders, London.

Ho, T.H., N. Charlet-B, M.G. Poulos, G. Singh, M.S. Swanson, and T.A. Cooper. 2004. Muscleblind proteins regulate alternative splicing. *EMBO J*. 23:3103-3112.

Huichalaf, C., Sakai, K., Jin, B., Jones, K., Wang, G.-L., Schoser, B., … Timchenko, L. (2010). Expansion of CUG RNA repeats causes stress and inhibition of translation in myotonic dystrophy 1 (DM1) cells. *FASEB journal. 24*(10), 3706–19.

Hunter, A., C. Tsilfidis, G. Mettler, P. Jacob, M. Mahadevan, L. Surh, and R. Korneluk. 1992. The correlation of age of onset with CTG trinucleotide repeat amplification in myotonic dystrophy. *J.Med.Genet.* 29:774-779.

Ikezoe, K., Nakamori, M., Furuya, H., Arahata, H., Kanemoto, S., Kimura, T., … Kira, J. (2007). Endoplasmic reticulum stress in myotonic dystrophy type 1 muscle. *Acta neuropathologica*, *114*(5), 527–35

Jiang, H., A. Mankodi, M.S. Swanson, R.T. Moxley, and C.A. Thornton. 2004. Myotonic dystrophy type 1 is associated with nuclear foci of mutant RNA, sequestration of muscleblind proteins and deregulated alternative splicing in neurons *Human Molecular Genetics*. 13:3079-3088.

Kaliman, P., and E. Llagostera. 2008. Myotonic dystrophy protein kinase (DMPK) and its role in the pathogenesis of myotonic dystrophy 1. *Cell.Signal.* 20:1935- 1941.

Kalsotra, A., Xiao, X., Ward, A. J., Castle, J. C., Johnson, J. M., Burge, C. B., & Cooper, T. a. (2008). A postnatal switch of CELF and MBNL proteins reprograms alternative splicing in the developing heart. *PNAS. 105*(51), 20333–8.

Kanadia, R. N., Johnstone, K. a, Mankodi, A., Lungu, C., Thornton, C. a, Esson, D., … Swanson, M. S. (2003). A muscleblind knockout model for myotonic dystrophy. *Science. 302*(5652), 1978–80.

Kanadia, R. N., Shin, J., Yuan, Y., Beattie, S. G., Wheeler, T. M., Thornton, C. a, & Swanson, M. S. (2006). Reversal of RNA missplicing and myotonia after muscleblind overexpression in a mouse poly(CUG) model for myotonic dystrophy. *PNAS. 103*(31), 11748–53.

Kimura, T., Nakamori, M., Lueck, J. D., Pouliquin, P., Aoike, F., Fujimura, H., … Sakoda, S. (2005). Altered mRNA splicing of the skeletal muscle ryanodine receptor and sarcoplasmic/endoplasmic reticulum Ca2+-ATPase in myotonic dystrophy type 1. *Human molecular genetics. 14*(15), 2189–200.

Koshelev, M., S. Sarma, R.E. Price, X.H. Wehrens, and T.A. Cooper. 2010. Heart-specific overexpression of CUGBP1 reproduces functional and molecular abnormalities of myotonic dystrophy type 1. *Human molecular genetics.* 19:1066-1075.

Kuyumcu-Martinez, N.M., G.S. Wang, and T.A. Cooper. 2007. Increased steady- state levels of CUGBP1 in myotonic dystrophy 1 are due to PKC-mediated hyperphosphorylation. *Mol.Cell.* 28:68-78.

Lam, L.T., Y.C. Pham, T.M. Nguyen, and G.E. Morris. 2000. Characterization of a monoclonal antibody panel shows that the myotonic dystrophy protein kinase, DMPK, is expressed almost exclusively in muscle and heart. *Hum.Mol.Genet.* 9:2167-2173.

Langlois, M. (2003). Hammerhead ribozyme-mediated destruction of nuclear foci in myotonic dystrophy myoblasts. *Molecular Therapy*, *7*(5), 670–680.

Lee, E.-S., Yoon, C.-H., Kim, Y.-S., & Bae, Y.-S. (2007).The double-strand RNA-dependent protein kinase PKR plays a significant role in a sustained ER stress-induced apoptosis. *FEBS letters*, *581*(22), 4325–32.

Lee, H. Y., Zhou, K., Smith, A. M., Noland, C. L., & Doudna, J. a. (2013). Differential roles of human Dicer-binding proteins TRBP and PACT in small RNA processing. *Nucleic acids research*, 1–9.

Lee, Jerome E, Lee, J. Y., Wilusz, J., Tian, B., & Wilusz, C. J. (2010). Systematic analysis of cis-elements in unstable mRNAs demonstrates that CUGBP1 is a key regulator of mRNA decay in muscle cells. *PloS one*, *5*(6), e11201.

Lee, Johanna E, Bennett, C. F., & Cooper, T. a. (2012). RNase H-mediated degradation of toxic RNA in myotonic dystrophy type 1. *PNAS. 109*(11), 4221–6.

Lee, Johanna E, & Cooper, T. (2009). Pathogenic mechanisms of myotonic dystrophy. *Biochemical Society transactions*, *37*(Pt 6), 1281–6.

Lin, X., J.W. Miller, A. Mankodi, R.N. Kanadia, Y. Yuan, R.T. Moxley, M.S. Swanson, and C.A. Thornton. 2006. Failure of MBNL1-dependent post-natal splicing transitions in myotonic dystrophy. *Human molecular genetics.* 15:2087-2097.

Liquori, C.L., K. Ricker, M.L. Moseley, J.F. Jacobsen, W. Kress, S.L. Naylor, J.W. Day, and L.P. Ranum. 2001. Myotonic dystrophy type 2 caused by a CCTG expansion in intron 1 of ZNF9. *Science.* 293:864-867.

Liu, G., Chen, X., Gao, Y., Lewis, T., Barthelemy, J., & Leffak, M. (2012). Altered replication in human cells promotes DMPK (CTG)(n) · (CAG)(n) repeat instability. *Molecular and cellular biology*, *32*(9), 1618–32.

Logigian, E.L., W.B. Martens, R.T. Moxley 4th, M.P. McDermott, N. Dilek, A.W. Wiegner, A.T. Pearson, C.A. Barbieri, C.L. Annis, C.A. Thornton, and R.T. Moxley 3rd. 2010. Mexiletine is an effective antimyotonia treatment in myotonic dystrophy type 1 *Neurology.* 74:1441-1448.

Magaña, J. J., & Cisneros, B. (2011). Perspectives on gene therapy in myotonic dystrophy type 1. *Journal of neuroscience research*, *89*(3), 275–85.

Mankodi, A., E. Logigian, L. Callahan, C. McClain, R. White, D. Henderson, M. Krym, and C.A. Thornton. 2000. Myotonic dystrophy in transgenic mice expressing an expanded CUG repeat. *Science.* 289:1769-1773.

Mankodi, A., Takahashi, M. P., Jiang, H., Beck, C. L., Bowers, W. J., Moxley, R. T., … Thornton, C. a. (2002). Expanded CUG repeats trigger aberrant splicing of ClC-1 chloride channel pre-mRNA and hyperexcitability of skeletal muscle in myotonic dystrophy. *Molecular cell*, *10*(1), 35–44.

Mankodi, A., Teng-Umnuay, P., Krym, M., Henderson, D., Swanson, M., & Thornton, C. a. (2003). Ribonuclear inclusions in skeletal muscle in myotonic dystrophy types 1 and 2. *Annals of neurology*, *54*(6), 760–8.

Marques, J. T., White, C. L., Peters, G. a, Williams, B. R. G., & Sen, G. C. (2008). The role of PACT in mediating gene induction, PKR activation, and apoptosis in response to diverse stimuli. *Journal of interferon & cytokine research. 28*(8), 469–76.

Masuda, A., Andersen, H. S., Doktor, T. K., Okamoto, T., Ito, M., Andresen, B. S., & Ohno, K. (2012). CUGBP1 and MBNL1 preferentially bind to 3' UTRs and facilitate mRNA decay. *Scientific reports*, *2*, 209.

Melo, S., Villanueva, A., Moutinho, C., Davalos, V., Spizzo, R., Ivan, C., & Rossi, S. (2011). Small molecule enoxacin is a cancer-specific growth inhibitor that acts by enhancing TAR RNA-binding protein 2-mediated microRNA processing. Mirkin, S. M. (2007). Expanda DNA repeats and human disease. *Nature*, *447*(7147), 932–40.

Miller, J.W., C.R. Urbinati, P. Teng-Umnuay, M.G. Stenberg, B.J. Byrne, C.A. Thornton, and M.S. Swanson. 2000. Recruitment of human muscleblind proteins to (CUG)(n) expansions associated with myotonic dystrophy. *EMBO J*. 19:4439-4448.

Mounsey, J.P., D.J. Mistry, C.W. Ai, S. Reddy, and J.R. Moorman. 2000. Skeletal muscle sodium channel gating in mice deficient in myotonic dystrophy protein kinase. *Human molecular genetics*. 9:2313-2320.

Mulders, S. a M., van Engelen, B. G. M., Wieringa, B., & Wansink, D. G. (2010). Molecular therapy in myotonic dystrophy: focus on RNA gain-of-function. *Human molecular genetics*. *19*(R1), R90–7.

Napierala, M., and W.J. Krzyzosiak. 1997. CUG repeats present in myotonin kinase RNA form metastable "slippery" hairpins. *J.Biol.Chem.* 272:31079-31085.

Noland, C. L., & Doudna, J. a. (2013). Multiple sensors ensure guide strand selection in human RNAi pathways. *RNA. 19*(5), 639–48.

Okoli, G., N. Carey, K.J. Johnson, and D.J. Watt. 1998. Over expression of the murine myotonic dystrophy protein kinase in the mouse myogenic C2C12 cell line leads to inhibition of terminal differentiation. *Biochem.Biophys.Res.Commun*. 246:905-911.

Otten, A.D., and S.J. Tapscott. 1995. Triplet repeat expansion in myotonic dystrophy alters the adjacent chromatin structure. *PNAS*. 92:5465- 5469.

Perrimon, N. & Mathey-Prevot, B. Applications of high-throughput RNA interference screens to problems in cell and developmental biology. *Genetics*. 175, 7–16 (2007).

Philips, A.V., L.T. Timchenko, and T.A. Cooper. 1998. Disruption of splicing regulated by a CUG-binding protein in myotonic dystrophy. *Science*. 280:737-741.

Ranum, L.P., and T.A. Cooper. 2006. RNA-mediated neuromuscular disorders. *Annu.Rev.Neurosci.* 29:259-277.

Ranum, L.P., P.F. Rasmussen, K.A. Benzow, M.D. Koob, and J.W. Day. 1998. Genetic mapping of a second myotonic dystrophy locus. *Nat.Genet*. 19:196-198.

Rau, F., Freyermuth, F., Fugier, C., Villemin, J.-P., Fischer, M.-C., Jost, B., … Charlet-Berguerand, N. (2011). Misregulation of miR-1 processing is associated with heart defects in myotonic dystrophy. *Nature structural & molecular biology*, *18*(7), 840–5.

Rhodes, J. D., Lott, M. C., Russell, S. L., Moulton, V., Sanderson, J., Wormstone, I. M., & Broadway, D. C. (2012). Activation of the innate immune response and interferon signalling in myotonic dystrophy type 1 and type 2 cataracts. *Human molecular genetics*, *21*(4), 852–62.

Savkur, R.S., A.V. Philips, and T.A. Cooper. 2001. Aberrant regulation of insulin receptor alternative splicing is associated with insulin resistance in myotonic dystrophy Nat.Genet. 29:40-47.

Shan, G., Li, Y., Zhang, J., Li, W., Szulwach, K. E., Duan, R., … Jin, P. (2008). A small molecule enhances RNA interference and promotes microRNA processing. *Nature biotechnology*, *26*(8), 933–40.

Singh, M., Fowlkes, V., Handy, I., Patel, C. V, & Patel, R. C. (2009). Essential role of PACT-mediated PKR activation in tunicamycin-induced apoptosis. *Journal of molecular biology*, *385*(2), 457–68.

Singh, M., & Patel, R. C. (2012). Increased interaction between PACT molecules in response to stress signals is required for PKR activation. *Journal of cellular biochemistry*, *113*(8), 2754–64.

Smith, K.P., M. Byron, C. Johnson, Y. Xing, and J.B. Lawrence. 2007. Defining early steps in mRNA transport: mutant mRNA in myotonic dystrophy type I is blocked at entry into SC-35 domains. *J.Cell Biol.* 178:951-964.

Suominen, T., L.L. Bachinski, S. Auvinen, P. Hackman, K.A. Baggerly, C. Angelini, L. Peltonen, R. Krahe, and B. Udd. 2011. Population frequency of myotonic dystrophy: higher than expected frequency of myotonic dystrophy type 2 (DM2) mutation in Finland *Eur.J.Hum.Genet.*

Takahashi, T., Miyakawa, T., Zenno, S., Nishi, K., Tanokura, M., & Ui-Tei, K. (2013). Distinguishable In Vitro Binding Mode of Monomeric TRBP and Dimeric PACT with siRNA. *PloS one*, *8*(5), e63434.

Tian, B, White, R. J., Xia, T., Tian, B. I. N., White, R. J., Xia, T., … Thornton, C. A. (2000). Expanded CUG repeat RNAs form hairpins that activate the double-stranded RNA-dependent protein kinase PKR. *RNA.* 6:79–87.

Tian, Bin, Mukhopadhyay, R., & Mathews, M. B. (2005). Polymorphic CUG repeats in human mRNAs and their effects on gene expression. *RNA biology*, *2*(4), 149–56.

Timchenko, L.T., N.A. Timchenko, C.T. Caskey, and R. Roberts. 1996. Novel proteins with binding specificity for DNA CTG repeats and RNA CUG repeats: implications for myotonic dystrophy. *Human molecular genetics*. 5:115-121.

Thornton, C.A., J.P. Wymer, Z. Simmons, C. McClain, and R.T. Moxley 3rd. 1997. Expansion of the myotonic dystrophy CTG repeat reduces expression of the flanking DMAHP gene *Nat.Genet.* 16:407-409.

Vignaud, A., A. Ferry, A. Huguet, M. Baraibar, C. Trollet, J. Hyzewicz, G. Butler-Browne, J. Puymirat, G. Gourdon, and D. Furling. 2010. Progressive skeletal muscle weakness in

transgenic mice expressing CTG expansions is associated with the activation of the ubiquitin-proteasome pathway. *Neuromuscul.Disord.* 20:319-325.

Wang, G.S., D.L. Kearney, M. De Biasi, G. Taffet, and T.A. Cooper. 2007. Elevation of RNA-binding protein CUGBP1 is an early event in an inducible heart- specific mouse model of myotonic dystrophy. *J.Clin.Invest.* 117:2802-2811.

Wang, G.S., M.N. Kuyumcu-Martinez, S. Sarma, N. Mathur, X.H. Wehrens, and T.A. Cooper. 2009. PKC inhibition ameliorates the cardiac phenotype in a mouse model of myotonic dystrophy type 1. *J.Clin.Invest.* 119:3797-3806.

Wansink, D.G., R.E. van Herpen, M.M. Coerwinkel-Driessen, P.J. Groenen, B.A. Hemmings, and B. Wieringa. 2003. Alternative splicing controls myotonic dystrophy protein kinase structure, enzymatic activity, and subcellular localization. *Mol.Cell.Biol.* 23:5489-5501.

Ward, A. J., Rimer, M., Killian, J. M., Dowling, J. J., & Cooper, T. a. (2010). CUGBP1 overexpression in mouse skeletal muscle reproduces features of myotonic dystrophy type 1. *Human molecular genetics*, *19*(18), 3614–22.

Warf, M. B., Nakamori, M., Matthys, C. M., Thornton, C. a, & Berglund, J. A. (2009). Pentamidine reverses the splicing defects associated with myotonic dystrophy. *PNAS*, *106*(44), 18551–6.

Wheeler, T.M., and C.A. Thornton. 2007. Myotonic dystrophy: RNA-mediated muscle disease. *Curr.Opin.Neurol*. 20:572-576.

Wheeler, T. M., Sobczak, K., Lueck, J. D., Osborne, R. J., Lin, X., Dirksen, R. T., & Thornton, C. a. (2009). Reversal of RNA dominance by displacement of protein sequestered on triplet repeat RNA. *Science*, *325*(5938), 336–9.

Wiles, A.M., Ravi, D., Bhavani, S. & Bishop, A.J. An analysis of normalization methods for Drosophila RNAi genomic screens and development of a robust validation scheme. *J. Biomol. Screen*. 13, 777–784 (2008).